Cell Communication and Signaling

RESEARCH

Open Access

REG3A secreted by peritumoral acinar cells enhances pancreatic ductal adenocarcinoma progression via activation of EGFR signaling

Xiaojing Ren[1†], Yunfei Teng[2†], Kunxin Xie[3†], Xiao He[2,4], Gang Chen[2,4], Kaini Zhang[5], Qingyi Liao[6], Jia Zhang[3], Xiaohang Zhou[3], Yating Zhu[3], Wenyu Song[3], Yuege Lin[2], Yi Zhang[7], Zhijian Xu[6], Noriaki Maeshige[8], Xiubin Liang[5], Dongming Su[2*], Peng Sun[3*] and Ying Ding[4*]

Abstract

Background Regenerating family member 3A (REG3A) is involved in the development of multiple malignant tumors, including pancreatic ductal adenocarcinoma (PDAC). However, any role of REG3A in PDAC remains controversial due to its unclear tissue localization or direct receptors, and complex downstream signal transductions.

Methods Morphological analysis and public multi-omics data retrieval were was utilized to elucidate the tissue localization of REG3A in PDAC. To ascertain the pro-oncogenic role of secreted REG3A, experiments were conducted using in vitro PDAC cell lines and in vivo tumor formation assays in nude mice. A battery of investigative techniques, including RNA sequencing, phospho-kinase arrays, western blot analyses, in silico docking simulations, gene truncation strategies, and co-immunoprecipitation, were employed to delve into the downstream signaling transduction pathways induced by REG3A.

Results In this study, we confirmed an association between increased serum levels of REG3A and poor prognosis in patients with PDAC. Morphological staining and bioinformatic analysis showed that REG3A was mainly expressed in peritumoral acinar cells that were spatially close to tumor region, while it was almost negative in PDAC tumor cells. Peritumoral REG3A expression levels, but not tumoral REG3A, were highly correlated with PDAC progression. Further in vitro experiments including RNA sequencing and molecular biological assays revealed that secreted REG3A could directly bind to the epidermal growth factor receptor (EGFR), an important pro-oncogene involved in cellular proliferation, and subsequently activate the downstream mitogen-activated protein kinase (MAPK) signals to promote PDAC tumor cell growth.

Conclusion Taken together, our data indicated that increased expression of REG3A in peritumoral acinar cells acts as a specific event to indicate PDAC progression, and verified EGFR as a possible target of REG3A, providing mechanistic insights into the role of REG3A, the diagnostic method and therapeutic strategy of PDAC.

†Xiaojing Ren, Yunfei Teng and Kunxin Xie contributed equally to this work.

*Correspondence:
Dongming Su
sudongming@njmu.edu.cn
Peng Sun
sunpeng@njmu.edu.cn
Ying Ding
dingying@njmu.edu.cn
Full list of author information is available at the end of the article

Keywords REG3A, Pancreatic ductal adenocarcinoma, Peritumoral acinar cell, Epidermal growth factor receptor (EGFR), Paracrine

Introduction

Pancreatic ductal adenocarcinoma (PDAC), with a 5-year survival of less than 10%, is among the most lethal of all cancers [1]. Due to the lack of early diagnosis, the majority of patients lose the opportunity for surgery and have poor prognosis. Tissue injury and some somatic mutations, such as the KRAS oncogene and the tumor suppressor genes CDKN2A, TP53, and SMAD4, are considered major reasons for tumor initiation and maintenance [2]. However, the molecular mechanisms of PDAC progression are complex and remain largely unknown. Further exploration of novel potential targets would benefit the diagnosis and clinical therapies of PDAC.

Among the potential molecular targets, the regenerating (REG) family members, which are secreted C-type lectins, have multiple biological roles in anti-inflammatory, tissue repair, cell proliferation, and apoptosis functions [3]. Five REG family members, REG1A, REG1B, REG3A, REG3G, and REG4, have been identified in humans [4], and their potential roles in tumorigenesis have been demonstrated in an increasing number of studies. REG3A, also known as hepatocarcinoma-intestine-pancreas (HIP) or pancreatic-associated protein (PAP), shows selective expression in gastrointestinal organs, including the pancreas [3], and was initially identified as a pancreatic inflammatory marker in pancreatitis [5]. More recently, REG3A was found to play key roles in both pancreatic islet cell regeneration in diabetes [6] and pancreatic carcinogenesis through the promotion of cancer cell proliferation, migration, and invasion [7–9]. Thus, REG3A could serve as a potential target for treatment or the diagnosis of PDAC.

Any role of REG3A in PDAC remains controversial due to its unclear tissue localization and complex downstream signal transductions. More importantly, all possible REG3A receptors have not yet been confirmed. Some molecules, such as exostoses-like gene 3 (EXTL3), have been identified to bind to REG3A in keratinocytes [10] and some other cell lines [7]. However, as EXTL3 mainly functions as a glycosyltransferase during heparin and heparan sulfate synthesis on the endoplasmic reticulum or Golgi apparatus [11], this function does not fully explain the mechanism of REG3A-induced transmembrane signal transduction in cells. Therefore, further investigations are needed to confirm the mechanisms of REG3A in the initiation and progression of PDAC.

In this study, we identified that REG3A was mainly expressed in peritumoral acinar cells that were spatially closed to tumor region, and its expression there was associated with the progression of PDAC. Further in vitro, in vivo, and bioinformatic analysis revealed that the secreted REG3A may stimulate the growth of PDAC cell lines by directly binding to the extracellular domain of epidermal growth factor receptor (EGFR), an important pro-oncogene involved in cellular proliferation [12], and this binding subsequently activated downstream mitogen-activated protein kinase (MAPK) signals in PDAC cells. These novel findings have added to the knowledge of the mechanisms by which REG3A may affect tumor growth and suggested REG3A as a potential target for use in the diagnosis and treatment of PDAC.

Materials and methods

Clinical data analysis

All analyses using human subjects were approved by the Institutional Ethics Committee of the First Affiliated Hospital of Nanjing Medical University. In total, 60 patients diagnosed with PDAC and 15 healthy volunteers were enrolled in this study. In the patients with PDAC, serum samples were obtained before surgery. The concentration of serum REG3A was measured using a commercial ELISA kit (RayBiotech, Norcross, GA, US). The median value was used as the low and high cut-offs to define the REG3A low and REG3A high groups. Overall survival (OS) was defined as the time from surgery to death. The characteristics of the patients with PDAC are listed in Supplementary Table S1.

Immunohistochemical staining

Immunohistochemical staining was performed using surgically resected tissue sections from the cohort of patients with PDAC listed in Supplementary Table S1, or on tissue microarrays (TMAs) containing 58 primary PDAC and corresponding adjacent pancreatic tissue specimens (SuperChip, Shanghai, China; the characteristics are listed in Supplementary Table S2). Primary antibodies used for immunohistochemical staining were: REG3A (#ab220884, Abcam, Cambridge, UK), p-STAT3 (#ab76315, Abcam), CK7 (#ab9021, Abcam), KI67 (#ab15580, Abcam). The integral optical density (IOD) of immunostaining was calculated using Image J software (National Institutes of Health, Bethesda, MA, US).

TCGA and GEO data retrieval

Raw RNA sequencing data were downloaded from a total of 146 confirmed PDAC cases from The Cancer Genome

Atlas (TCGA) and 171 pancreas samples from GTEx Data. The expression of REG3A between PDAC tumors and normal pancreas tissues was analyzed using the R Limma package [13]. GEO data sets (GSE71989, GSE43795, GSE101448, GSE62165, GSE28735, GSE62452, and GSE32676. Detailed information is listed in Supplementary Table S3) containing tumor and non-tumor samples were obtained from the National Center for Biotechnology Information's (NCBI) Gene Expression Omnibus (GEO, http://www.ncbi.nlm.nih.gov/geo/). The expression of REG3A in each data set was ranked, and the median was taken as the cutoff point. All patients were then classified into a low- or high-expression group to analyze the effect of REG3A expression on survival rates. The differences in biological processes and signaling pathways between the high and low REG3A groups were analyzed using the gene ontology (GO) [14] or Kyoto Encyclopedia of Genes and Genomes (KEGG) pathways [15].

Single-cell RNA sequencing (scRNA-seq) and spatial transcriptomic data retrieval

The scRNA-seq expression matrix (GSE155698 [16], GSE202051 [17], GSE141017 [18], and CRA001160 [19]) was processed using the R package Seurat [20]. The gene expression data were normalized, and 2,000 differentially expressed genes (DEGs) were identified. UMAP reduction was used for cluster visualization, and the R package ggplot2 was used to visualize gene expression. For the spatial transcriptomic data (GSE111672 [21]), the R package Seurat was used to obtain the spatial location of the cells in different clusters.

Using the Slingshot algorithm with default parameters, a pseudo-time trajectory analysis was performed to arrange cells into a developmental trajectory, which was segmented with different branches to imitate cell evolution or differentiation. The R package TradeSeq [22] and Monocle2 [23]. was used to analyze the sequencing data based on the developmental trajectories of the cells; the data were fitted into a negative binomial generalized additive model (GAM) for each gene, and an inference was performed on the parameters of the GAM. The expression of genes associated with the pseudo-time or along the trajectory was marked. Copy number variations (CNVs) were inferred using the R package inferCNV [24]. CNVs in the sex and mitochondrial chromosomes were excluded from the analysis. PySCENIC package [25] was used to calculate the transcription factor activity between different cell clusters in scRNA-seq datasets.

Cell culture and REG3A overexpression

Human pancreatic cancer cell lines (PANC-1, AsPC-1, BxPC-3, and SW1990), the rat AR42J amphicrine pancreatic cell line, and Chinese hamster ovary (CHO) cells were obtained from Shanghai Cell Bank, Chinese Academy of Sciences, or American Type Culture Collection (ATCC, Manassas, VA, US). The AsPC-1 cells were cultured in RPMI-1640 medium; the other cell lines were cultured in Dulbecco's modified Eagle's medium (DMEM); both media also contained 10% FBS and 1% penicillin/streptomycin. The cell lines were confirmed to be free of *Mycoplasma* contamination by short tandem repeat (STR) analysis using a commercial kit (TransGen Biotech, Beijing, China). All cells were cultured in a 37 °C incubator with 5% CO_2. For stable infection, adenoviral vectors (AdVec), adenoviral human REG3A (AdREG3A), or adenoviral human REG3A lacking the signal peptide sequence (1–26 amino acid deletion, AdΔREG3A) were constructed by Vigene Biosciences (Jinan, China). Overexpression of REG3A in cell lines was performed using adenovirus according to its instruction.

Western blot analysis

After treatment, the cells were washed with PBS and lysed in RIPA buffer (Beyotime Biotechnology, Shanghai, China) supplemented with protease and phosphatase inhibitors (Thermo Fisher Scientific, Waltham, MA, US). Western blot analysis was performed as previously described [26]. Briefly, protein lysates were separated on 8%–12% SDS polyacrylamide gels and then transferred to polyvinylidene difluoride (PVDF) membranes. After blocking with bovine serum albumin (BSA), the membranes were incubated with anti-REG3A (#ab192224, Abcam, Cambridge, UK), anti-tubulin (#2128, Cell Signaling Technology, Danvers, MA, US), anti-phosphorylated STAT3 (#9131, Cell Signaling Technology), anti-STAT3 (#4904, Cell Signaling Technology), anti-phosphorylated tyrosine (#9411, Cell Signaling Technology), anti-phosphorylated EGFR (Y1068, #3777, Cell Signaling Technology), anti-EGFR (#4405, Cell Signaling Technology), anti-phosphorylated ERK (#4370, Cell Signaling Technology), or anti-ERK (#4695, Cell Signaling Technology) antibodies. The secondary antibody was HRP-conjugated anti-rabbit IgG (#111-035-003, Jackson ImmunoResearch Labs, West Grove, PA, US). For the phospho-kinase array, a commercial MAPK pathway phosphorylation array (#AAH-MAPK-1-4, RayBiotech, Norcross, GA, US) was used following the manufacturer's protocol. Unless otherwise specified, all protein phosphorylation detection were performed in cells under serum-starved conditions for 24 h. Image J software (National Institutes of Health, Bethesda, MD, US) was used to measure the integrated optical density (IOD) of each dot. All blots were repeated at least 3 times for the statistical analysis.

To detect EGFR dimerization, PANC-1 cells were starved in serum-free medium for 24 h, washed with PBS, and then cold PBS containing 10 ng/mL recombinant human EGF (SinoBiological, Beijing, China) or 1 μg/mL recombinant human REG3A (rhREG3A, SinoBiological) was added to the plates, which were then incubated for 30 min at 4 °C. The cells were again washed with cold PBS and then incubated with 0.5 mM bis(sulfosuccinimidyl) suberate cross-linker (BS3, Thermo Fisher Scientific) in PBS for 2 h at 4 °C on ice. After washing again, the cross-linking reaction was stopped by incubating in 50 mM Tris buffer (pH 7.5) for 15 min. The cells were then lysed, and the dimerization of EGFR was analyzed by western blotting.

Co-Immunoprecipitation (Co-IP)

PANC-1 cells were treated with 10 μg/mL rhREG3A or vehicle for 1 h, then were washed with PBS and ruptured with lysis buffer (Beyotime). The extracted proteins were used as input or for further immunoprecipitation analysis. Briefly, the proteins were firstly incubated with anti-REG3A antibodies for 2 h and then mixed with Protein G beads overnight (Beyotime). The beads were collected by a magnetic stand and washed. The immunoprecipitated products were resuspended and used for further immunoblots.

Real-time PCR assay

Total RNA extraction and real-time PCR assay were performed as previously described [27]. The relative expression of REG3A mRNA was calculated and normalized to the housekeeping gene Gapdh. Primer sequences were: Reg3a (F: CCTGACGAACATCCCAGATCA, R: GGG AGTCTTCACCTCGTACC), Gapdh (F: TGGGAAGCT GGTCATCAAC, R: GCATCACCCCATTTGATGTT).

Cell viability, colony formation, transwell cell invasion assay, and ELISA assays

Cell viability was detected using the Cell Counting Kit-8 (CCK8, #C0037, Beyotime, Shanghai, China), as previously described [28]. For colony formation, cells were plated in 6-well plates, given the desired treatment for one week, and the resulting colonies were fixed with 4% paraformaldehyde and stained with 0.2% crystal violet (Beyotime). The colonies were counted using ImageJ software. For transwell cell invasion assay, cells were plated in a transwell plate with Matrigel Matrix (354, 234, Corning, US) on top of the transwell membrane, the cell invasion was measured as previously described [28]. For colony formation, 5 replicated wells were analyzed ($n=5$). For invasion assay, at least 10 random sights in 5 replicated wells were selected to analyze the proliferative ratios for each group ($n=5$). All experiments were repeated at least 3 times.

The concentration of REG3A secreted into the culture medium was determined using a commercial ELISA kit (RayBiotech). The data were adjusted based on the corresponding protein concentrations.

Immunofluorescence and EdU staining

Cell immunofluorescence studies were performed as previously described [29]. Briefly, after the experimental treatment, the cells were fixed in 4% paraformaldehyde for 2 h, followed by incubation with anti-REG3A (#ab220884, Abcam), anti-EGFR (sc-373746, Santa Cruz Biotechnology, CA, USA), and anti-Calnexin (#ab213243, Abcam) primary antibodies, and then with Alexofluor 488/594-conjugated IgGs (#A-11034/11037, Invitrogen, Carlsbad, CA, US). Nuclei were stained with DAPI. The cell proliferative ratios were measured using an EdU staining kit (Beyotime). Images were captured using a DP70 microscope (Olympus, Tokyo, Japan). ImageJ software was used to calculate the proliferative ratio for each group. At least 10 random sights in 5 replicated wells were selected to analyze the proliferative ratios for each group ($n=5$). All experiments were repeated at least 3 times.

Luciferase reporter gene assay

Truncated REG3A promoters (-2000–0, -100–0) were cloned forward of the luciferase reporter gene, which was co-transfected with human STAT3 vectors into HEK-293 T cells. The Luciferase Reporter Assay System (Promega, Fitchburg, WI, USA) was used to measure the transcriptional activity as previously described [30].

MicroScale thermophoresis (MST) assay

The direct binding activity of rhREG3A to EGFR extracellular domain or intracellular kinase domain (SinoBiological) was detected by the MicroScale thermophoresis assay. Briefly, the MonolithTM RED-NHS kit (Cat# MO-L011, NanoTemper, South San Francisco, CA, USA) was used according to the manufacturer's protocols.

In vivo tumor formation

Six-week-old female BALB/C nude mice were obtained from Cavens Lab Animal (Changzhou, China). All animal experiments were approved by the Institutional Animal Care and Use Committee of Nanjing Medical University. Cultured cells (5×10^6 PANC-1 or AsPC-1 cells), either stably overexpressing REG3A or treated with adenoviral vector, were resuspended in 1:1 PBS/Matrigel (#356237, Corning) and injected into the right flank of the mice. Tumor size was measured weekly and calculated using

the following equation: length × width × width. Four weeks after cell injection, the mice were euthanized by CO_2 and the tumor tissues were removed.

RNA sequencing

Cells were plated in 6-well plates, treated with 1 μg/mL rhREG3A or vehicle for 24 h, and then harvested for RNA extraction. Library construction and transcriptome sequencing were performed by Genedenovo Biotechnology Co., Ltd. (Guangzhou, China) on an Illumina HiSeq™ 2500 system. After quality control and alignment with rRNA, the removed rRNA reads of each sample were mapped to the reference genome using TopHat2 [31]. The gene expression level was normalized using the fragments per kilobase of exon model per million mapped reads (FPKM). Differentially expressed genes (DEGs) were identified across groups using the edgeR package (http://www.rproject.org/). Genes with a fold change ≥ 2 and a false discovery rate (FDR) < 0.05 in a comparison were identified as significant DEGs. GO/KO enrichment analyses were performed as already described. All RNA sequencing data were deposited in the Gene Expression Omnibus (GEO) database under accession number GSE282763.

In silico modeling of REG3A-EGFR complexes

The structures of human REG3A (PDB ID: 1UV0) and EGFR (PDB ID: 1MOX) were downloaded from the PDB database [32, 33]. Two protein structures were prepared by removing water molecules and heteroatoms and minimizing energy. Docking experiments for REG3A and EGFR were performed in ClusPro [34–37], which allows for moderate conformational changes. The program uses the fast Fourier transform (FFT) correlation method to sort samples using knowledge-based or statistical potentials as a scoring function to select the best model of the complex [38]. The docking solutions were evaluated based on the model scores. The placement of each residue was deduced from accessibilities and executed "by hand" in a PyMOL session. The interaction diagrams were produced with Ligplot + [39] and PDB sum [40] based on the refined model.

Statistical analysis

Data are presented as the mean ± SD. A paired t test, two-tailed unpaired Student's t test, or one-way analysis of variance (ANOVA) followed by Dunnett's posttest were conducted to compare the statistical difference among the different groups. For Kaplan–Meier survival curves, the log-rank test was used to assess statistical significance. $P < 0.05$ indicates significant difference.

Results

Higher peritumoral but not tumoral REG3A expression indicates malignant progression and poor prognosis in patients with PDAC

As shown in Fig. 1A, serum REG3A concentration was higher in patients with PDAC than in healthy individuals, and much higher serum REG3A levels were observed in patients with high-grade TNM stages of PDAC. In this present cohort, an elevated serum REG3A level (> 15 ng/mL) has an accuracy of 78.0% and a specificity of 73.3% for diagnosing PDAC (Fig. 1A. Supplementary Table 1). The survival outcomes were worse for patients with high (52.8 ± 16.1 ng/mL) serum REG3A levels than with low (16.5 ± 8.7 ng/mL) serum REG3A levels (Fig. 1B).

The in situ expression of REG3A in a TMA containing 58 primary PDAC and corresponding adjacent pancreatic tissue specimens (Figure S1A) revealed almost no REG3A immunostaining in the tumoral areas of the sections. Instead, most of the immunostaining was evident in the corresponding adjacent pancreatic tissues, which showed varying levels of REG3A staining (Fig. 1C, D, S1A). Four samples in this TMA appeared to show higher REG3A expression in the tumoral region than in the corresponding normal peritumoral region on this TMA (Fig. 1C, S1B); however, a reevaluation of the tissue morphology confirmed strict localization of REG3A expression in the peritumoral tissues (Figure S1C). More importantly, survival was shorter in the patients with higher peritumoral REG3A expression than with low expression (Fig. 1E). This suggested an association between higher peritumoral REG3A expression and poor prognosis in patients with PDAC but no similar association for tumoral REG3A expression.

We then analyzed the public transcriptomic data of patients with PDAC available in the TCGA, GTEx, and GEO database. In line with the data from our own samples, the mRNA expression of REG3A was significantly lower in PDAC tumor tissues from the public data set than in peritumoral tissues or normal pancreas (Fig. 1F). In two public data sets (GSE28735 and GSE62452) containing corresponding peritumoral samples and complete prognosis data [41, 42], patients with higher peritumoral REG3A expression also had worse survival outcomes, while tumoral REG3A expression did not indicate prognosis (Fig. 1G). Furthermore, to obtain the role of peritumoral REG3A at a single-cell resolution, we subsequently collected three single-cell sequencing data sets, CRA001160, GSE155698, and GSE202051, from patients with PDAC and one single-cell GSE141017 sequencing data set from K-ras$^{LSL.G12D/+}$; Trp53$^{R172H/+}$; Pdx-1-Cre (KPC) mice, as REG3A expression could be identified in some cell cohorts from those data sets. Similar to the results obtained from morphological staining

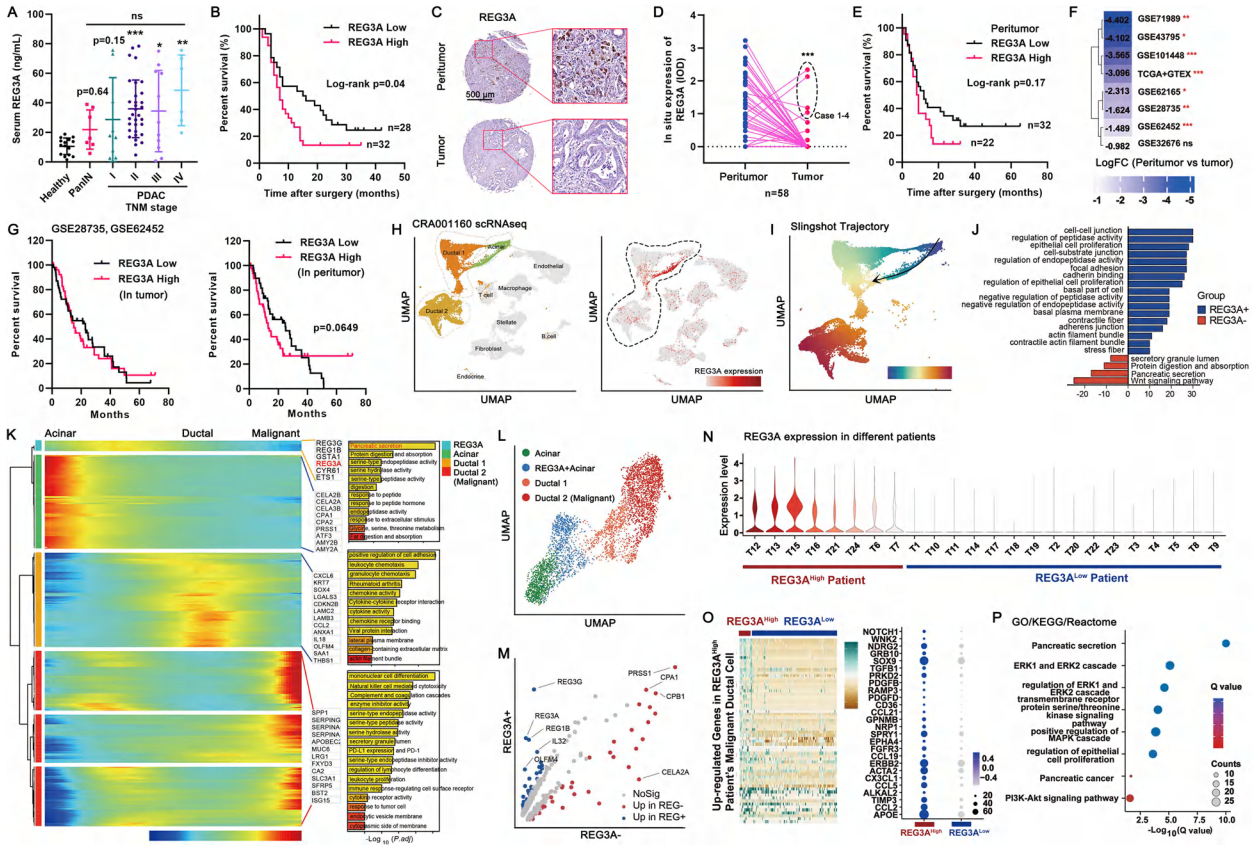

Fig. 1 Higher peritumoral REG3A expression indicates malignant progression and poor prognosis in patients with PDAC. **A** The serum concentration of REG3A in healthy volunteers and patients with different TNM stages of PDAC. **B** The median value was used as the low and high cut-offs to define the REG3A-Low ($n=28$) and REG3A-High ($n=32$) groups. Kaplan–Meier survival analysis of patients with different serum REG3A levels. **C** Representative images of REG3A expression in a tissue microarray (TMA) cohort of PDAC specimens. **D** The integral optical density (IOD) analysis of in situ REG3A expression from the TMA PDAC specimens with 54 paired (peritumor vs tumor) samples. **E** Kaplan–Meier survival analysis of patients with different peritumoral REG3A expression levels (REG3A-Low, $n=32$; REG3A-High, $n=22$) in the TMA cohort. **F** The expression of REG3A in tumor tissues compared to peritumoral tissues in patients with PDAC from the TCGA, GTEx, and GEO database. Peritumoral tissue number vs tumor tissue number: TCGA and GTEx (171 vs 179), GSE71989 (8 vs 14), GSE43795 (5 vs 6), GSE101448 (19 vs 24), GSE62165 (13 vs 118), GSE28735 (45 vs 45, paired), GSE62452 (69 vs 69, paired), GSE32676 (7 vs 25). $^{*}p<0.05$, $^{**}p<0.01$, $^{***}p<0.001$, ns = not significant, in different data sets. **G** Kaplan–Meier survival analysis of patients with different tumoral or peritumoral REG3A expression levels from the GSE28735 and GSE62452 data sets. **H**-**P** Single cells RNA sequencing analysis using CRA001160 data set. **H** UMAP representation of different subgroups; the expression levels of REG3A in each subgroup were plotted onto the UMAP. **I** Pseudo-time reconstitution of acinar and ductal cells with abnormal gene expression profiles and malignant ductal cells inferred by slingshot trajectory. **J** The KO/GO enrichment analysis between REG3A-positive and REG3A-negative acinar cells. **K** The heatmap view of trajectory in the slingshot trajectory. Color key indicates low to high expression levels. **L** The different cell clusters of the acinar and ductal cells. (M) The DEGs between REG3A-positive and REG3A-negative acinar cell clusters. **N** The expression of REG3A in different patients with PDAC from the CRA001160 cohort. **O** The up-regulated genes in the malignant ductal cells from the patients with higher acinar cell REG3A expression compared to patients with low acinar cell REG3A expression. **P** The GO/KEGG/Reactome pathway enrichment of up-regulated genes in (**O**)

in our TMA cohorts, REG3A was more highly expressed in acinar cells than in malignant ductal cells or other types of cells (Fig. 1H, Figure S2A-S2C). We then conducted an in-depth analysis of a data set (CRA001160) containing large numbers of acinar cells and a pseudo-time reconstitution of acinar cells and ductal cells with abnormal (ductal 1) and malignant (ductal 2) gene expression profiles (Fig. 1H). Along the slingshot trajectory, the expression of malignant markers, was gradually increased, while the genes that indicates normal acinar cell function, such as pancreatic enzyme carboxypeptidase A1 (CPA1), were decreased with the progression of PDAC (Fig. 2I-M). During this trajectory, REG3A expression was activated during the acinar-to-ductal metaplasia (ADM) stage when the cells exhibited more malignant epithelioid features, while the expression of REG3A quickly decreased when accompanied by the loss of acinar cell function genes, such as CPA1 (Fig. 2I-M).

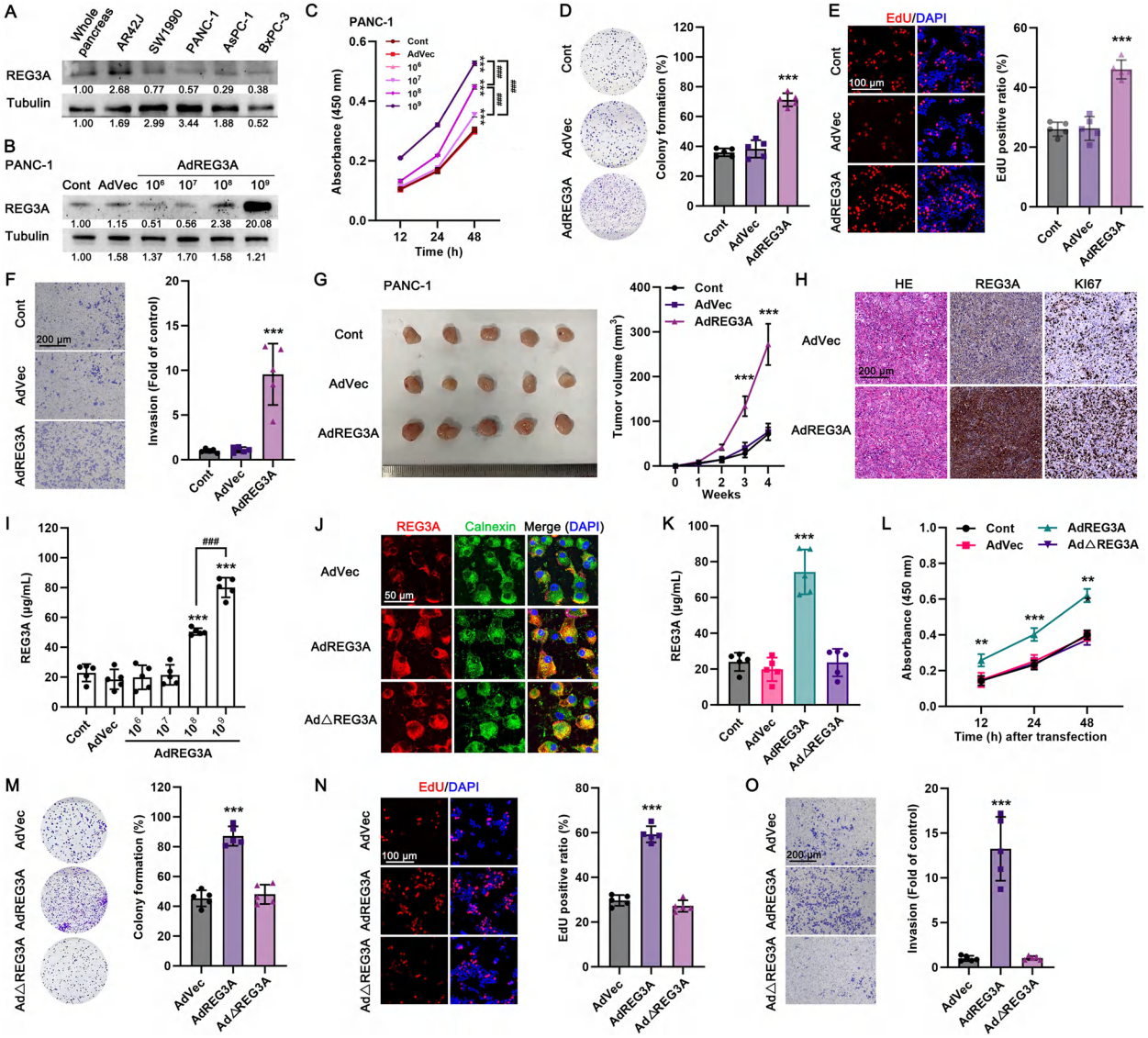

Fig. 2 REG3A promotes in vitro and in vivo PDAC tumor growth. **A** The expression of REG3A in human pancreas tissue, rat AR42J cells, and human SW1990, PANC-1, AsPC-1, and BxPC-3 pancreatic cancer cell lines. **B** The PANC-1 cells were infected with a REG3A adenovirus overexpression vector (AdREG3A) or vector alone (AdVec), and expression of REG3A was determined by western blotting. All blots were repeated at least 3 times; tubulin was used as the internal reference. **C** At different times after infection, the cell viability of PANC-1 cells was measured. ***$p < 0.001$ compared to the Control group, ###$p < 0.001$ as indicated, $n = 5$. **D** After infection with 10^9 AdREG3A or AdVec for 1 week, PANC-1 cell colonies were stained with crystal violet, and the colony numbers were counted. **E** After infection with 10^9 AdREG3A or AdVec for 48 h, EdU staining was performed to assess the proliferative ratio in the different groups. **F** After infection with 10^9 AdREG3A or AdVec for 48 h, cell invasion was measured by transwell assay. **G** Photograph of PANC-1 xenograft tumors at 4 weeks after cell injection; The in vivo tumor volume was recorded after PANC-1 cell injection. ***$p < 0.001$ compared to the Control group, $n = 5$. **H** The xenograft tumor sections were stained with H&E dye, anti-REG3A, or anti-KI67 antibodies. Scale bar = 200 μm, and referred to all panels. **I** The concentration of REG3A in the culture medium 48 h after infection. ***$p < 0.001$ compared to the Control group, ###$p < 0.001$ as indicated, $n = 5$. **J** PANC-1 cells infected with 10^9 AdREG3A, AdVec, or REG3A sequence lacking the signal peptide (AdΔREG3A) and immunostained with anti-REG3A (red) or anti-Calnexin (green) antibodies; nuclei were stained with DAPI. Scale bar = 50 μm, and refers to all panels. **K** After infection with 10^9 AdREG3A, AdVec, or AdΔREG3A for 48 h, the concentration of REG3A in the culture medium was measured. ***$p < 0.001$ compared to the Control group, $n = 6$. **L**-**O** After infection, the cell viability, colony formation, EdU staining, invasion of PANC-1 cells were determined, **$p < 0.01$, ***$p < 0.001$ compared to the AdVec group, $n = 5$

Similar results were also found using the GSE141017 data set from KPC mice (Figure S2D-S2I). We subsequently identified the expression of REG3A in the acinar cells from the individual patients in CRA001160 cohort (Fig. 1N), and found that the expression of genes in ductal epithelial cells that related to malignant

progression was enriched in patients with higher REG3A expression in acinar cells (Fig. 1O and P).

REG3A promotes in vitro and in vivo PDAC tumor growth

As peritumoral REG3A is highly correlated with PDAC progression, we further investigate the effect of REG3A on in vitro cultured PDAC cell lines. Figure 2A and S3A show lower expression of REG3A in SW1990, PANC-1, AsPC-1, or BxPC-3 pancreatic cancer cell lines than in pancreas tissue or the rat AR42J amphicrine pancreatic cell line. However, following adenovirus-mediated overexpression of REG3A (Fig. 2B, Figure S3B, S4A-S4B), the cell viability, colony formation, cell proliferation, and invasion were greater in the REG3A-overexpressing cells than in vector-treated cells (Fig. 2C-F, Figure S4). The in vivo subcutaneous xenograft model using PANC-1 or AsPC-1 cells also showed that adenovirus-mediated overexpression of REG3A stimulated tumor growth in nude mice (Fig. 2G, Figure S3G) with a higher proliferative ratio (Fig. 2H). Pathological analysis and bioinformatic retrieval suggested that peritumoral REG3A may play roles in tumor growth through paracrine mechanisms. We next investigated this possible effect of secreted REG3A in vitro. Moreover, the REG3A concentration in the culture medium was increased by AdREG3A treatment in a dose-dependent manner (Fig. 2I). PANC-1 cells with overexpressed REG3A were further subjected to immunofluorescent staining, and REG3A was co-localized with calnexin, an endoplasmic reticulum marker (Fig. 2J). When the sequence of the signal peptide of REG3A was removed, the secreted REG3A in the cultured medium was obviously lost (Fig. 2K). As expected, the AdΔREG3A could not stimulate PANC-1 tumor cell growth in vitro (Fig. 2L-O). These data suggested that REG3A could acted as a typical secreted protein.

EGFR-MAPK activation is involved in the proliferative effect of secreted REG3A on PDAC cells

As a secreted protein, we next investigated the effect of recombinant human REG3A (rhREG3A) on PANC-1 cells. When PANC-1 cells were treated with rhREG3A protein, the cell viability, colony formation, cell proliferation, and invasion were all enhanced (Fig. 3A-D), as well as in AsPC-1, BxPC-3, and SW1990 PDAC cell lines (Figure S3I, S3L-S3M), strongly suggesting that REG3A promotes tumor growth via a paracrine (PDAC tumor growth in vivo)/autocrine (REG3A overexpressed pancreatic cancer cells in vitro) model. Mechanically, the transcriptomic data of rhREG3A protein-stimulated and vehicle-treated PANC-1 cells identified 343 upregulated and 165 downregulated DEGs (Fig. 3E, F). The upregulated DEGs mainly included genes that related to EGFR-MAPK signaling pathways (Fig. 3G), GO/KEGG enrichment, PPI, and GSEA analysis also indicated the activation of some oncogenic signaling pathways, including the EGF/EGFR and MAPK signaling pathways, by REG3A stimulation (Fig. 3H-K).

REG3A activates EGFR signaling pathways through direct binding to the extracellular domain of EGFR

These above results strongly suggested that EGFR activating could be associated with the effect of REG3A. Further assessment of the acute effect of rhREG3A on signaling pathways in PANC-1 cells using a phospho-kinase array and a 30 min treatment with rhREG3A resulted in the activation of the MAPK pro-proliferative pathway, including the phosphorylation of MEK S217/221, p53 S15, and RSK1 S380, and a weak phosphorylation of ERK T202/204 and Y185/187 (Fig. 4A).

MAPK signaling is activated by some cytokines, including EGF [12], we further found rhREG3A activated phosphorylated tyrosine kinase within the molecular weight range of approximately 150–200 kDa; Conversely, the expressions of pTYR residues below 100 kDa were relatively unaltered by rhREG3A treatment (Fig. 4B). Subsequently, REG3A stimulated the phosphorylation of EGFR (Y1068) and the downstream phosphorylation of ERK in a time-dependent manner (Fig. 4C). Similar to the effect of EGF, the natural ligand of EGFR, rhREG3A also induced endogenous EGFR dimerization (Fig. 4D). Co-immunoprecipitation and double immunofluorescent staining showed a co-localization between REG3A and EGFR in exogenous rhREG3A-stimulated PANC-1 cells (Fig. 4E and F). Further MST assay confirmed a direct binding of rhREG3A to the extracellular domain (ECD) of EGFR protein in vitro (Fig. 4G). For reference, co-incubation with the EGFR inhibitor cetuximab, the tyrosine kinase inhibitor afatinib, or the MEK inhibitor PD98059, effectively suppressed rhREG3A-induced EGFR-ERK activation (Figure S5, S6).

Therefore, the possible ligand-dependent EGFR activation by REG3A was verified in CHO cells that did not express EGFR. Overexpression using an EGFR plasmid in these CHO cells (Fig. 5A) revealed a time-dependent activation of the EGFR-ERK pathway due to rhREG3A expression similar to the effects observed in the PANC-1 pancreatic cancer cell line (Fig. 5B, C). However, rhREG3A stimulation altered CHO-Vec cells less in comparison with CHO-EGFR cells (Figure S7). Further in silico analysis suggested that the region of REG3A required for EGFR binding was identified by unconstrained dockings with ClusPro, which output the top 10 docking REG3A–EGFR complexes for model scores. A conclusive result was retained (cluster center: -672.5, lowest energy:

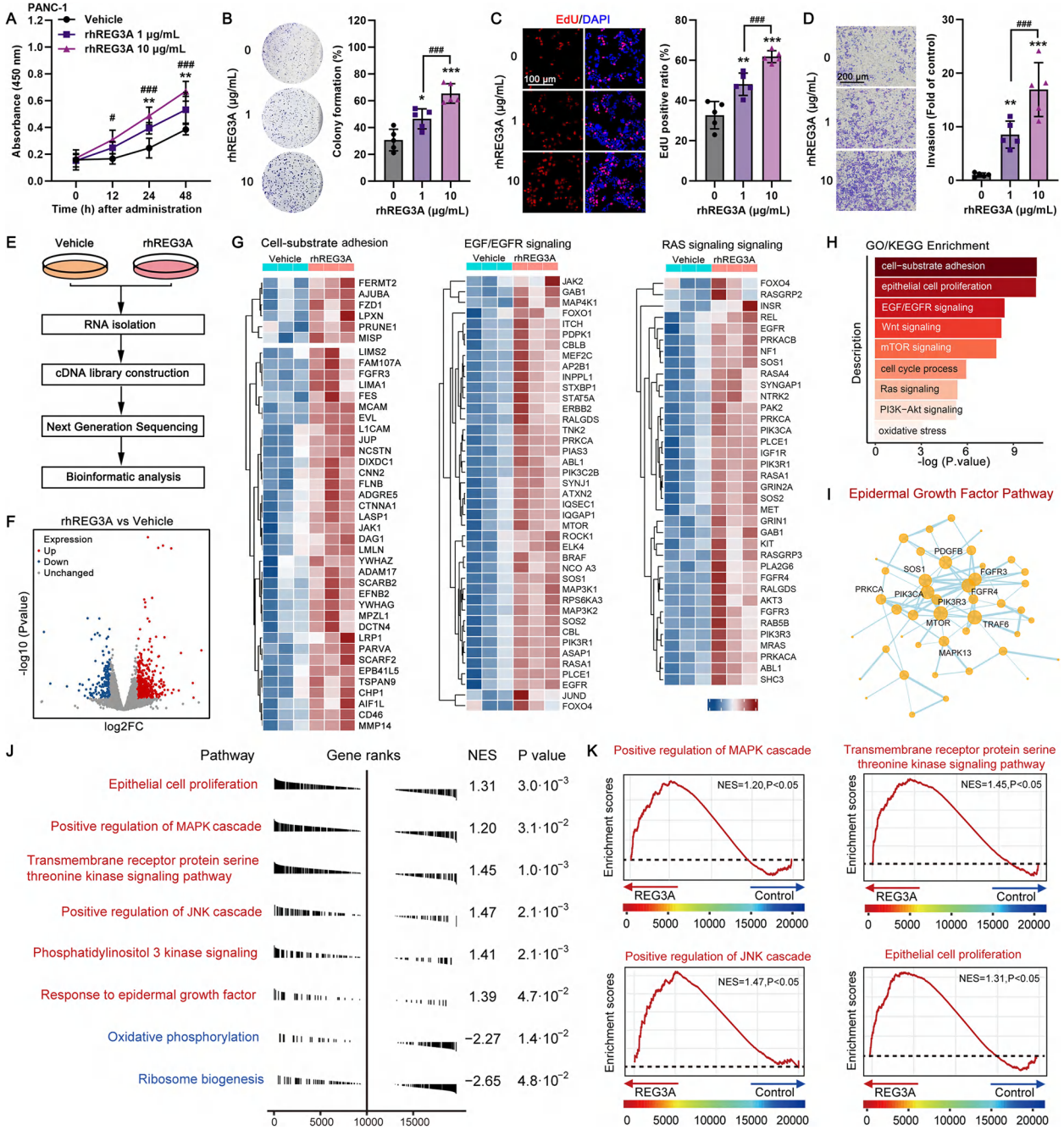

Fig. 3 Recombinant REG3A stimulates PANC-1 cell growth via EGFR-MAPK pathways. **A**-**D** PANC-1 cells were treated with different concentrations of recombinant human REG3A (rhREG3A) for different durations and the cell viability, colony formation, EdU staining, and cell invasion were determined, $^{**}p < 0.01$, $^{***}p < 0.001$ in 1 μg/mL group, $\#p < 0.05$, $\#\#p < 0.01$, $\#\#\#p < 0.001$ in 10 μg/mL group, compared to the vehicle-treated group, $n = 5$. **E** PANC-1 cells were treated with 10 μg/mL rhREG3A for 24 h, total RNA was isolated and RNA sequencing was performed. **F** Volcano plot showing the upregulated and downregulated genes in PANC-1 cells treated with 10 μg/mL rhREG3A for 24 h. **G** Heatmap showing the representative upregulated genes in rhREG3A-treated PANC-1 cells. **H** GO/KEGG enrichment analysis showing upregulated pathways in rhREG3A-treated PANC-1 cells. **I** Protein–protein interaction (PPI) analysis was performed using upregulated genes in the epidermal growth factor (EGF) pathway. **J** Gene set enrichment analysis (GSEA) of the upregulated genes in rhREG3A-treated PANC-1 cells. **K** Representative GSEA curves in (**J**)

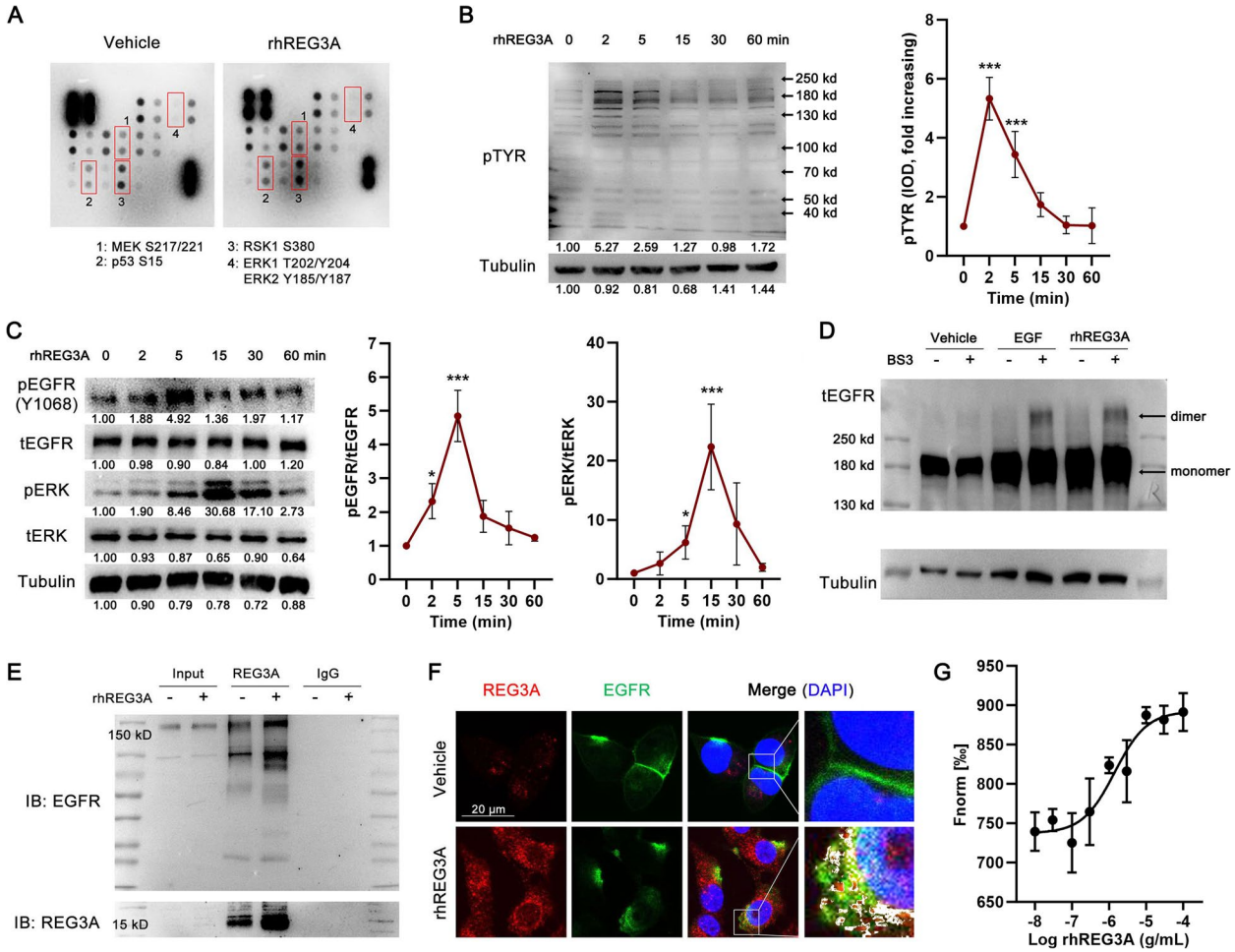

Fig. 4 EGFR-MAPK activation is involved in the proliferative effect of REG3A in PDAC cells. **A** Phosphokinase array analysis of PANC-1 cells serum starved for 24 h, followed by 10 μg/mL rhREG3A or vehicle treatment for 30 min. Dot blots are shown, with altered dots marked by red frames. **B** Phosphorylation of tyrosine kinase and **C** phosphorylation of EGFR and ERK detected by western blots of PANC-1 cells serum starved for 24 h, followed by 10 μg/mL rhREG3A treatment for different times. **D** Dimerization assay performed using the BS3 cross-linker, followed by western blot analysis using EGFR antibody in PANC-1 cells serum starved for 24 h, followed by 10 μg/mL rhREG3A or 100 ng/mL EGF treatment for 30 min. All blots were repeated at least 3 times; tubulin was used as an internal reference; the integrated optical density (IOD) of each band in the independent blot was analyzed (*$p < 0.05$, ***$p < 0.001$, compared to 0-time, $n = 3$). **E** The PANC-1 cells were treated with vehicle or 10 μg/mL rhREG3A for 1 h, then the cells were lysed for Co-immunoprecipitation (Co-IP). **F** Double immunofluorescent staining of REG3A (red) and EGFR (green), in vehicle or rhREG3A-simulated PANC-1 cells, DAPI (blue) was used to stain nuclei, white marker indicated the co-localization of REG3A and EGFR (yellow), scale bar = 20 μm. **G** The in vitro binding activity of rhREG3A to the extracellular domain of EGFR protein by MST assay

(See figure on next page.)

Fig. 5 REG3A activates EGFR by direct binding to the extracellular domain of EGFR. **A** CHO cells were transfected with human EGFR or vector plasmids, and the expression of EGFR was confirmed. **B** CHO cells transfected with EGFR plasmid (CHO-EGFR) were starved for 24 h, and stimulated with 10 μg/mL rhREG3A for different times and evaluated for phosphorylation of EGFR and ERK by western blotting. **C** All blots were repeated at least 3 times; tubulin was used as an internal reference; the integrated optical density (IOD) of each band in the independent blot was analyzed (*$p < 0.05$, **$p < 0.01$, ***$p < 0.001$, compared to 0-time, $n = 3$). **D** Schematic representation of the three-dimensional structure of a predicted REG3A–EGFR complex (illustrated with PyMOL). Red, full length of human REG3A; Cyan, the extracellular domain of EGFR (PDB ID: 1MOX). **E** Ligplot + diagram showing the protein residues that interact between REG3A (chain B) and EGFR (chain A). **F** Interaction plots for a predicted REG3A–EGFR complex. Residue colors: Gray, aliphatic (Ile, Ala, Leu, Val), blue, alkaline (Arg, Lys), orange (Gly, Pro), violet, aromatic (Tyr, Phe), yellow (Cys), red (Asp), green (Gln, Ser, Asn, Thr). Plot of H-bonds (blue lines), salt bridges (red lines), and non-bonded contacts (orange tick marks) between residues on either side of the REG3A-EGFR complex interface. **G** Schematic representation of the three-dimensional structure of a predicted EGFR ligand–EGFR complex (illustrated with PyMOL). Red, full length of different human EGFR ligands; Cyan, the extracellular domain of EGFR (PDB ID: 1MOX)

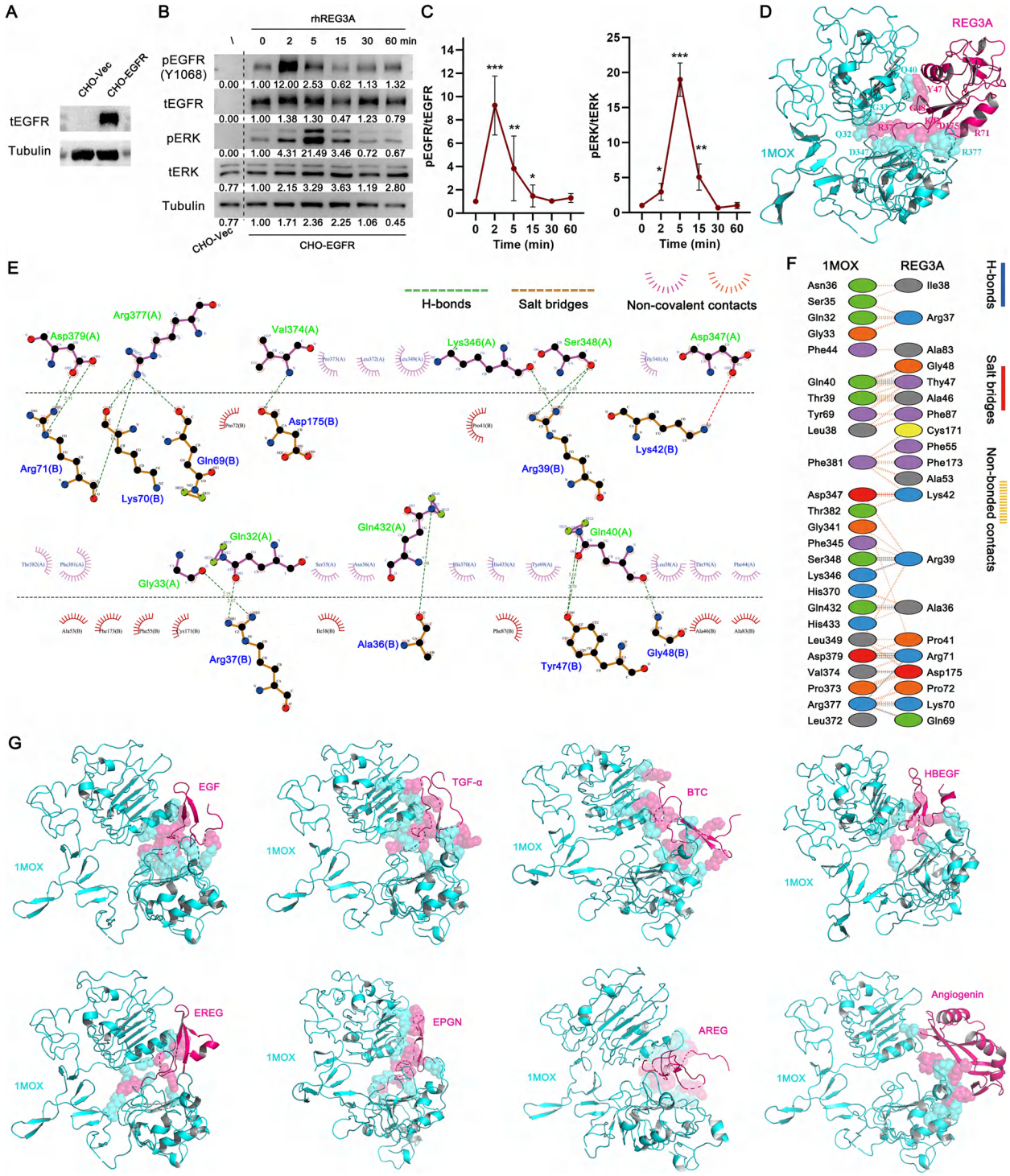

Fig. 5 (See legend on previous page.)

-753.1 kcal/mol), and REG3A was localized in the structural architecture of the domain I (L1) and III (L2) sites on the extracellular region of EGFR (Fig. 5D-F), which was most similar to the classical binding site of EGF compare to other reported EGFR ligands (Fig. 5G).

To identify the region of REG3A required for EGFR binding, we deleted the C-terminal C-type lectin domain

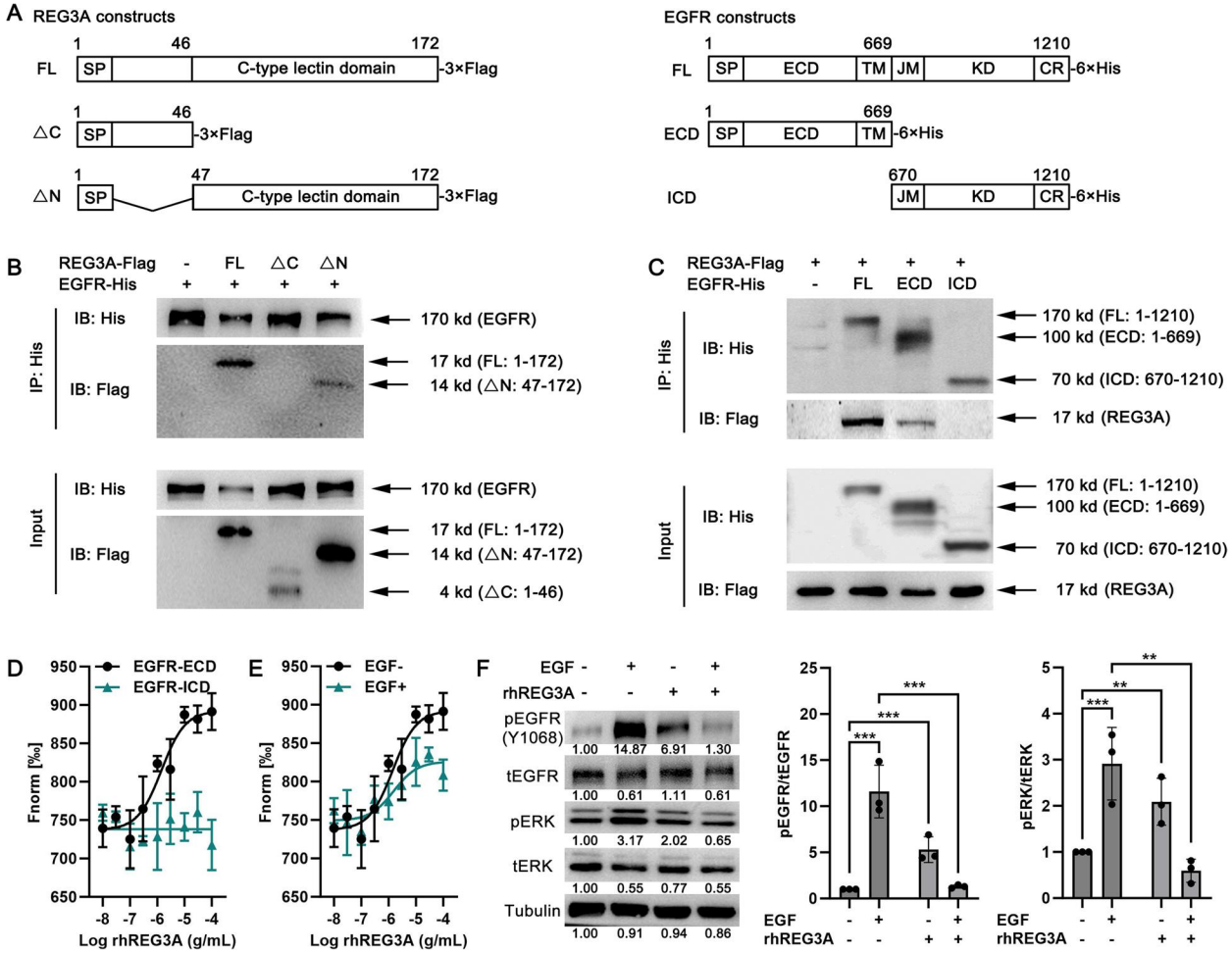

Fig. 6 REG3A binds to EGFR-ECD region, requiring its C-type lectin domain. **A** Schematic diagram of full-length (FL), C-terminal deletion (△C), N-terminal deletion (△N) constructs of Flag-REG3A; FL, extracellular domain (ECD), intracellular domain (ICD) of His-EGFR; signal peptide (SP), transmembrane (TM), juxtamembrane (JM) regions, kinase domain (KD), C-terminal region (CR). **B**, **C** After the CHO cells were co-transfected with different REG3A/EGFR truncations, anti-His antibody immunoprecipitation (IP: His) was performed. Representative immunoblot of EGFR-His and REG3A-Flag in IP and in whole-cell lysate (input) is shown. **D** The in vitro binding activity of rhREG3A to the ECD or the ICD of EGFR protein by MST assay, $n = 3$. **E** The in vitro binding activity of rhREG3A to the ECD of EGFR protein in the presence/absence of 10 ng/mL EGF by MST assay, $n = 3$. **F** The PANC-1 cells were starved for 24 h, and treated with 10 ng/mL EGF in the present/absent of 10 μg/mL rhREG3A for 5 min, or different times, the phosphorylation of EGFR and ERK were determined by western blotting. All blots were repeated at least 3 times; tubulin was used as an internal reference; the integrated optical density (IOD) of each band in the independent blot was analyzed (**$p < 0.01$, ***$p < 0.001$, as indicated, $n = 3$)

(amino acids 47–172), or the N-terminal region of REG3A, while the EGFR-ECD and intracellular kinase domain (ICD) were also constructed (Fig. 6A). After the CHO cells were co-transfected with different truncated REG3A and EGFR plasmids, immunoprecipitation data showed that the deletion of C-type lectin domain obviously abolished the binding of REG3A to EGFR (Fig. 6B). In addition, REG3A tends to recognize EGFR-ECD, but not ICD truncation (Fig. 6C). By using MST assay, we confirmed that rhREG3A generates specific binding activity to the ECD of EGFR but not intracellular kinase domain (ICD, Fig. 6D); this binding activity and down-stream EGFR-ERK phosphorylation could be competitively inhibited by EGF (Fig. 6E, F), suggesting a direct binding of REG3A to EGFR at the pocket of the EGF-binding site.

Inflammatory signal-stimulated STAT3 activation contributes to the increased expression of REG3A in peritumoral acinar cells

To investigate the reasons for the specific up-regulated expression of REG3A in peritumoral acinar cells in PDAC, we performed PySCENIC analysis to find the

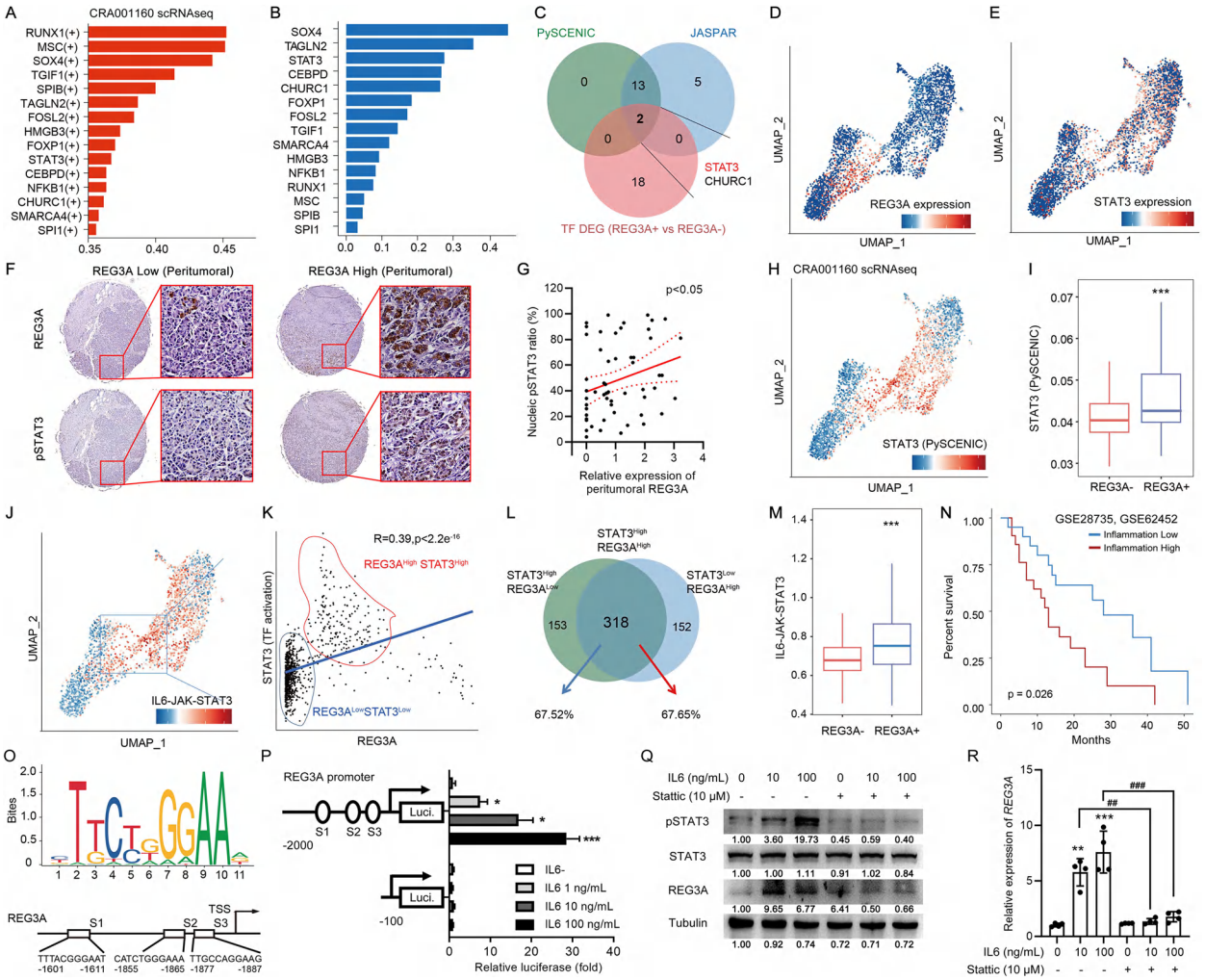

Fig. 7 Inflammation-mediated STAT3 activation contributes to the up-regulated REG3A expression in acinar cells. **A** PySCENIC analysis of activated transcriptional factors, **B** The up-regulated mRNAs of transcriptional factors in REG3A-positive acinar cells compared to REG3A-negative acinar cells in CRA001160 dataset. **C** The intersection of (**A**), (**B**), and the transcriptional factors with binding sites with the promoter region of REG3A predicted by JASPAR database. **D** The REG3A expression in Fig. 1L. **E** The mRNA expression of STAT3 in Fig. 1L. **F** The representative image of REG3A and phosphorylated STAT3 expression in the TMA cohort. **G** The relationship between peritumoral REG3A and phosphorylated STAT3 expression level in the TMA cohort. **H** The transcriptional activation of STAT3 prediction by PySCENIC analysis in Fig. 1L. **I** The transcriptional activation of STAT3 between REG3A-positive acinar cells and REG3A-negative acinar cells in CRA001160 dataset. **J** The IL6-JAK-STAT3 pathway activation of STAT3 prediction by PySCENIC analysis in Fig. 2J. **K** The relationship between REG3A expression and STAT3 activation in (**J**). **L** The intersection of STAT3-positive and REG3A-positive acinar cells. **M** The IL6-JAK-STAT3 pathway activation between REG3A-positive acinar cells and REG3A-negative acinar cells in CRA001160 dataset. **N** The survival outcomes between different levels of IL6-JAK-STAT3 pathway activation. **O** The binding sites of STAT3 in the promoter region of REG3A predicted by JASPAR. **P** The luciferase reporter gene assay under IL6-stimulation, $n = 3$. **Q** The AR42J cells were stimulated with different concentration of IL6 in the presence/absence of 10 μM Stattic for 24 h, the protein was extracted and the expression levels of phosphorylated STAT3, total STAT3, REG3A, and Tubulin were measured by western blot analysis, all blots were performed at least for three times. **R** The AR42J cell lines were stimulated with different concentration of IL6 in the presence/absence of 10 μM Stattic for 24 h, the mRNA level of REG3A was detected by qPCR assay, $^{***}p < 0.001$, $n = 4$

activated transcriptional factors in REG3A-positive acinar cell clusters (Fig. 7A). In combination with up-regulated transcriptional factors in the mRNA level (Fig. 7B) and the possible binding to the promoter region of REG3A genes, we found STAT3 was highly related to the up-regulation of REG3A (Fig. 7C). Using CRA001160 scRNA-seq dataset, we confirmed the higher expression of STAT3 mRNA in REG3A-positive acinar cells compared to REG3A-negative acinar cells (Fig. 7D, E). Immunostaining in the TMA cohort also revealed a significant positive-correlation between REG3A expression and nucleic phosphorylated STAT3

ratio in the peritumoral region of PDAC (Fig. 7F, G). Furthermore, STAT3 activation (Fig. 7H, I) and IL6-JAK-STAT3 pathway enrichment (Fig. 7J) both confirmed this speculation: activated STAT3 may contribute to the up-regulated transcription of REG3A in acinar cells. The IL6-JAK-STAT3 pathway activation was further confirmed in the likelihood analysis between STAT3- and REG3A-positive clusters (Fig. 7L, M). Mapping this IL6-JAK-STAT3 pathway to the bulk RNAseq datasets GSE28735 and GSE62452, the higher activation of IL6-JAK-STAT3 pathway significantly indicated poorer prognosis (Fig. 7N). In vitro luciferase reporter gene assay further confirmed the direct transcriptional activation of STAT3 on REG3A (Fig. 7O, P). In vitro IL6 dose-dependently stimulated STAT3 phosphorylation and increased REG3A expression; while STAT3 inhibitor, Stattic abolished IL6-induced STAT3 phosphorylation and further REG3A mRNA transcription (Fig. 7Q, R, S9).

REG3A specifically expresses in peritumoral acinar cells that were spatially close to the malignant PDAC cells to activate EGFR-MAPK signal

As REG3A expression was higher in the peritumoral region than in the tumoral region of PDAC tissue, we further investigated the detailed localization of REG3A-positive cells in the paraffin sections from surgically removed PDAC tissues. The morphological data brings strong visual impact: REG3A expression was strictly restricted to the normal acini or acinar-to-ductal metaplasia (ADM) region, but was almost negative in CK7-positive ductal adenocarcinoma cells; noticeably, there were fewer KI67-positive nuclei in the REG3A-positive acinar region compared to the adjacent CK7-positive ductal region (Fig. 8A, Figure S10). Further more, analysis of one sample with regional REG3A expression from the publicly available GSE111672 spatial transcriptome data set [21] allowed us to identify pancreatic exocrine, ductal epithelial, and tumor regions and to assign others as the stroma region (Figure S11). PRSS1 and FXYD3

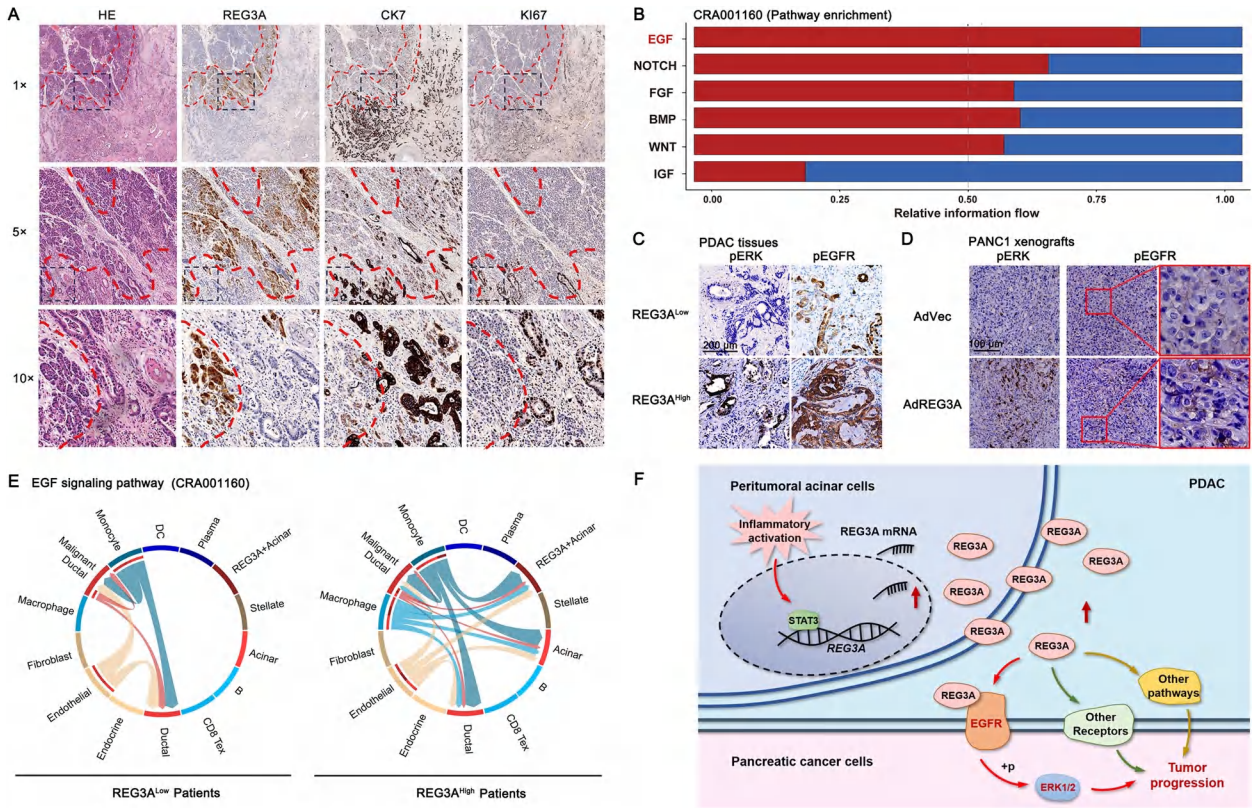

Fig. 8 Peritumoral acinar cell secreted REG3A activates EGFR-MAPK signal in PDAC. **A** The HE staining and immunohistochemical staining using REG3A, CK7, and KI67 antibodies in a same PDAC tissue with different magnifications. **B** Pathway enrichment in patients with high expression of REG3A in CRA001160 dataset. **C** Immunohistochemical staining of pERK and pEGFR in patients with different expression of REG3A (left) and vector or REG3A transfected PANC1 xenografts in nude mice (right). **E** Cell communications between different cell clusters in REG3A^{Low} and REG3A^{High} patients in CRA001160 dataset. **F** Graphic abstract. Inflammatory signals-stimulated STAT3 activation contributes to the increased REG3A expression in acinar cells, which then the secreted REG3A stimulates the growth of PDAC cell by activating EGFR signal directly

were used as markers of the exocrine and tumor regions, respectively (Figure S5B). We observed markedly higher expression of REG3A in the pancreatic exocrine region than in the other regions (Figure S11C). The epithelial cells with lower REG3A expression levels were also spatially localized close to the tumor tissues and had significantly higher CNVs than the cells with higher REG3A expression (Figure S11D). The expression of REG3A was also negatively correlated with malignant gene expression in epithelial cells (Figure S11E), suggesting that the expression patterns of REG3A could be associated with the malignant progression of ductal cells. In scRNA sequencing data (CRA001160), REG3A^{High} patients also possess higher EGF activation rate in malignant ductal cells (Fig. 8B), as well as enhanced expression of pERK and pEGFR levels were found in patients with REG3A^{High} PDAC (Fig. 8C), or in AdREG3A-PANC-1 xenografts (Fig. 8D) by immunohistochemical staining. Cell communication analysis further confirmed obvious difference in EGF signaling pathway between REG3A^{High} and REG3A^{Low} patients (Fig. 8E). These data together suggested that inflammatory signals-stimulated STAT3 activation contributes to the increased REG3A expression in acinar cells, which then the secreted REG3A stimulates EGFR-MAPK activation, and promotes PDAC cell growth (Fig. 8F).

Discussion

The proliferation-promoting effect of REG3A is commonly found in multiple cell types; for example, a cultured rat insulinoma cell line INS-1 cells in our previous study [6], human epidermal keratinocytes [10], and multiple cancer cell lines [43, 44]. Zhang et al. found that exogenous REG3A treatment induced ADM by activating classical mitogen-activated protein kinase (MAPK) signaling pathway, indicating a paracrine effect of REG3A in PDAC [7]. Thus, the direct effect of secreted REG3A as an onco-promoting paracrine factor in PDAC cells should be evaluated. Rosty et al. reported that only 1 (5%) of 19 pancreatic cancer cell lines expressed REG3A transcripts [45]. Our overexpression of REG3A in several PDAC cell lines revealed that only REG3A secreted into the medium could stimulate cell growth, and this was confirmed by the direct addition of recombinant REG3A protein. Together with previous overexpression or recombinant studies on pancreatic and other cancers, these data support the stimulation of PDAC cell growth, both in vitro and in vivo, by secreted REG3A.

However, although the involvement of several molecules has been reported in the elicitation of REG3A-related signals, the signaling pathway still remains controversial [46]. The potential receptors or REG3A-related molecules have been the focus of research on REG3A-related molecules in recent years. The use of protein-interaction technology has identified some proteins, such as EXTL3 [10] or fibronectin 1 [43], as possible functional REG3A receptors. EXTL3 is the most commonly mentioned molecule [3], but its action does not fully explain REG3A-related signals for at least two reasons: 1) As a secretory protein, REG3A most likely functions through classical ligand–receptor transmembrane signal transduction, especially in PDAC cells, according to our present data. However, EXTL3 mainly functions as a glycosyltransferase in heparin and heparan sulfate synthesis occurring in the endoplasmic reticulum or Golgi apparatus [11]; therefore, a function as a transmembrane receptor lacks evidence. Recently, Moniaux et al., reported that the interaction between REG3A and EXTL3 does not influence the glycosyltransferase activity of EXTL3 [47], offer further corroboration for the hypothesis that EXTL3/heparan sulfate may not serve as the primary mediator of REG3A's biological effects, especially in its proliferative capacity on tumor cells. 2) Protein–protein-interaction assays, such as co-immunoprecipitation assays, can recognize direct receptors, but they can also interact with multiple intracellular receptors during the synthesis and modification of a protein in the endoplasmic reticulum or Golgi apparatus. One possible explanation is that REG3A may affect interacting proteins, such as EXTL3 or fibronectin 1, to regulate some biological process involved in the production of intracellular or extracellular matrix (ECM), which would be biological effects that are distinct from transmembrane signal transduction. However, more evidence is needed.

Including REG3A, target identification currently represents a significant bottleneck in biological research. Recently, advancements in technologies such as single-cell RNA sequencing and other multi-omics approaches have afforded us the opportunity to investigate the potential interactions between REG3A and other proteins. In the present study, our use of RNA sequencing in recombinant REG3A-treated PDAC cells enriched only proliferative signals, whereas multiple MAPKs were activated by recombinant REG3A stimulation by using a phosphorylation array, suggesting an acute effect. The proliferation-promoting and anti-apoptotic effects of REG3A are widely accepted, and many recent studies support the activation of some signal pathways, such as MAPK [7] or JAK-STAT [8], by REG3A. Therefore, we view the possible activation of some transmembrane receptors, such as receptor tyrosine kinase family members, as one of the more likely explanations for REG3A effects. Some potential transmembrane receptors of REG3A have been reported. Pharmacological inhibition methods have identified glycoprotein 130 (gp130) as a co-receptor

that regulates REG3A-stimulated JAK-STAT signaling in PDAC cells [8, 9]. An immunoprecipitation study by Liu et al. indicated that REG3A activated JAK-STAT signaling in the SW1900 PDAC cell line, possibly by interacting with EGFR [48]. Although Zhang et al. found no interaction between gp130/EGFR and REG3b, a mouse homolog of human REG3A, in acinar cell lines [7], considering the importance of EGFR in the progression of PDAC and the developed EGFR-targeted therapy, for example, using of tyrosine kinase inhibitors (TKIs) in the treatment of unresectable PDAC [12], we evaluated this possibility by examining whether the MAPKs activated in PDAC cells by REG3A required direct activation of EGFR by using EGFR inhibitor cetuximab, tyrosine kinase inhibitor afatinib, and MEK inhibitor PD98059. Although these pharmacological inhibitions did not conclusively demonstrate that REG3A-stimulated tumor growth was specifically mediated through EGFR activation, combined with other data, it suggested that secreted REG3A possibly acts as a novel ligand of EGFR to activate the downstream signals responsible for its proliferation-promoting effects.

In addition to the natural ligand EGF, seven different growth factors—high-affinity ligand EGF, transforming growth factor alpha (TGF-α), betacellulin (BTC), and heparin binding EGF-like growth factor (HB-EGF); low-affinity ligands are epiregulin (EREG), epigen (EPGN), and amphiregulin (AREG)—have been identified as EGFR ligands, and each displays qualitatively and quantitatively different downstream signals [49]. Wang et al. also reported that angiogenin/ribonuclease 5 could act as an EGFR ligand in PDAC [49]. Noticeably, some c-type lectins were found to have affinities with EGFR [50, 51]. As REG3A also belongs to the c-type lectin family [52], our exploration of the specificity of this REG3A-EGFR reaction showed that REG3A induced a dimerization of EGFR similar to that induced by its natural ligand, EGF. Furthermore, in CHO cells that did not express endogenous EGFR [53], REG3A still activated EGFR-MAPK signaling after transfecting the CHO cells with human EGFR, but this effect was not observed in CHO cells transfected with vector control. In silico docking and further in vitro verification experiments suggested that REG3A may bind to sites on the I (L1) and III (L2) domains on the extracellular region of EGFR in a similar manner to that of classical binding by EGF, thereby promoting the dimerization of this important RTK in cells. Paracrine interactions play crucial roles in the progression of malignant tumors, and they rely on cell communication networks [54]. Expression of many genes, including REG3A, could be altered in the non-neoplastic parenchyma adjacent to infiltrating PDAC [55], as indicated by the strong expression of some important cancer markers, such as feto-acinar pancreatic protein (FAP), in the peritumoral acinar area but a lack of expression in tumors and normal organs [56]. More data from crystallography and molecular biology are still needed to establish the ligand–receptor relationship between REG3A and RTKs; however, this paracrine effect that leads to increased expression and secretion of REG3A in peritumoral acinar cells and promotion of PDAC progression through direct EGFR activation appears to provide a reasonable explanation for REG3A effects.

In addition, REG3A is a secretory protein, and recent studies have proposed using the serum REG3A level as a biomarker for the diagnosis of PDAC [9, 57–59]. The aim of the present study was originally to evaluate the level of serum REG3A in patients with PDAC. In accordance with previous studies, higher REG3A levels were detected in the serum from patients with PDAC, and were associated with poor prognosis. Interestingly, in the corresponding pathological sections, the expression of REG3A was essentially negative in tumor cells and was mainly detected in the peritumoral acinar cells. Some earlier studies demonstrated increased REG3A expression in PDAC tissues, as with most oncogenes [60, 61]. However, recent studies indicated that REG3A is mainly expressed in inflamed acinar cells [7, 9, 45]. Considering the important role of REG3A in pancreatitis, convincing evidence exists to establish a paracrine effect model involving REG3A secretion from peritumoral acinar cells in PDAC. Further exploration of the underlying mechanism will be valuable.

In the present study, we revealed that REG3A mainly expressed in peritumoral acinar cells, especially in those acinar cells that were spatially close to malignant tumor cells, but REG3A expression was almost negative in PDAC tumor cells by a series of high-quality immunostaining, tissue microarray evaluation, and bioinformatic analysis of datasets from different database including scRNA-seq and spatial transcriptomic analysis. We also identified the STAT3, a down-stream inflammatory activation transcriptional factor, may contributes to the up-regulated expression of REG3A in the peritumoral acinar cells. Our findings were in line with some previous studies [7, 9].

Zhang et al. suggested that in situ expression of REG3A in acinar cells was involved in the acinar-to-ductal metaplasia (ADM) process [7]. The relationship between ADM and the progression of PDAC has been well documented, as the process of ADM is associated with the loss of the exocrine function of the acinar cells, which transform into duct-like structures that no longer express acinar markers, such as carboxypeptidase A1 (CPA1), amylase, and elastase [62]. This transformation is a highly probable explanation for the negative expression of REG3A in PDAC tumor cells, as REG3A expression, like other acinar

markers, is lost in malignant transformed cells. Bioinformatic analysis using scRNA-seq data sets from patients with PDAC or KPC mice also showed a perfect pseudotime trajectory analysis result, supporting the idea that normal acinar cells could transition into malignant acinar cells with higher CNV, and then to ductal cells. Along this trajectory, REG3A presented a trend indicating an early increase and a later decrease, while the acinar markers, such as CPA1, decreased, and malignant ductal markers, such as CDK4, increased. Therefore, we also agree with the opinion that the expression of REG3A is a hallmark event in this malignant transformation: PanIN arises from acinar cells undergoing ADM and then progresses to invasive PDAC. Further studies using genetic editing in the KPC mouse model, including REG3A knock-in, knockout, or lineage tracing lines, would be valuable for a comprehensive assessment of the biological roles of REG3A in the progression of PDAC.

Conclusions

Therefore, our study provided strong evidence for the hypothesis: Increased expression of REG3A in peritumoral acinar cells acts as a specific pathological event to indicate PDAC progression; The acinar cell-secreted REG3A may stimulate the growth of PDAC cells by directly binding to EGFR and activating the down-stream MAPK signals. The findings presented here could have important clinical implications if REG3A can serve as a serum and pathological marker in the diagnosis of PDAC, or if treatments involving REG3A or EGFR-TKIs can improve targeted therapy for PDAC.

Abbreviations

REG3A	Regenerating family member 3A
PDAC	Pancreatic ductal adenocarcinoma
EGFR	Epidermal growth factor receptor
MAPK	Mitogen-activated protein kinase
OS	Overall survival
TMAs	Tissue microarrays
IOD	Integral optical density
GO	Gene ontology
KEGG	Kyoto Encyclopedia of Genes and Genomes
scRNA-seq	Single-cell RNA sequencing
DMEM	Dulbecco's modified Eagle's medium
BSA	Bovine serum albumin
CCK8	Cell Counting Kit-8
MST	MicroScale thermophoresis
PanIN	Pancreatic intraepithelial neoplasia
ADM	Acinar-to-ductal metaplasia
ECD	Extracellular domain
ICD	Intracellular kinase domain

Supplementary Information

The online version contains supplementary material available at https://doi.org/10.1186/s12964-025-02103-4.

Supplementary Material 1.

Authors' contributions

Y.D., P.S., and D.S. conceived and designed the study and interpreted the results. X.R., Y.T., X.H., G.C., K.Z., J.Z., X.Z., Y.L., and Y.Z. performed the experiments; K.X., Q.L., Y.Z., W.S., and Z.X. performed the bioinformatic and in silico analyses. N.M., and X.L. provided reagents and advice. P.S. wrote the manuscript with comments from all authors.

Funding

This work is supported by the National Natural Science Foundation of China (82172991, 81502089 to Y. Ding; 81603169 to P. Sun; 81570779, 81170252, 81070656 to D. Su; 81670619, 81870467 to X. Liang; 82302922 to Y. Zhang), the Natural Science Research Program for Higher Education in Jiangsu Province (21KJB320015 to Y. Ding) and National Key Research and Development Program of China (2022YFF0713005 to D. Su).

Data availability

All RNA sequencing data were deposited in the the GEO database under accession code GSE282763.

Declarations

Ethics approval and consent to participate

All analyses using human subjects were approved by the Institutional Ethics Committee of the First Affiliated Hospital of Nanjing Medical University (2021-SRFA-137). All animal experiments were approved by the Institutional Animal Care and Use Committee of Nanjing Medical University.

Consent for publication

Not applicable.

Competing interests

The authors declare no competing interests.

Author details

[1]Third Hospital of Shanxi Medical University, Shanxi Bethune Hospital, Shanxi Academy of Medical Sciences, Tongji Shanxi Hospital, Taiyuan 030032, China. [2]Department of Pathology, Nanjing Medical University, Nanjing 211166, China. [3]Key Laboratory of Human Functional Genomics of Jiangsu Province, Department of Biochemistry and Molecular Biology, Nanjing Medical University, Nanjing 211166, China. [4]Department of Pathology, the First Affiliated Hospital of Nanjing Medical University, Nanjing 210029, China. [5]Department of Pathophysiology, Nanjing Medical University, Nanjing 211166, China. [6]State Key Laboratory of Drug Research, Shanghai Institute of Materia Medica, Chinese Academy of Sciences, Shanghai 201203, China. [7]Department of Pathology, Jiangsu Cancer Hospital, Jiangsu Institute of Cancer Research, Nanjing Medical University Affiliated Cancer Hospital, Nanjing 210009, China. [8]Department of Rehabilitation Science, Kobe University Graduate School of Health Sciences, 7-10-2 Tomogaoka, Kobe, Hyogo 654-0142, Japan.

Received: 3 October 2024 Accepted: 10 February 2025
Published online: 18 February 2025

References

1. Mizrahi JD, Surana R, Valle JW, Shroff RT. Pancreatic cancer. Lancet. 2020;395:2008–20.
2. Gromisch C, Qadan M, Machado MA, Liu K, Colson Y, Grinstaff MW. Pancreatic adenocarcinoma: unconventional approaches for an unconventional disease. Cancer Res. 2020;80:3179–92.
3. Wang L, Quan Y, Zhu Y, Xie X, Wang Z, Wang L, Wei X, Che F. The regenerating protein 3A: a crucial molecular with dual roles in cancer. Mol Biol Rep. 2022;49:1491–500.
4. Chen Z, Downing S, Tzanakakis ES. Four decades after the discovery of regenerating Islet-Derived (Reg) proteins: current understanding and challenges. Front Cell Dev Biol. 2019;7:235.
5. De Caro A, Lohse J, Sarles H. Characterization of a protein isolated from pancreatic calculi of men suffering from chronic calcifying pancreatitis. Biochem Biophys Res Commun. 1979;87:1176–82.

6. Ding Y, Xu Y, Shuai X, Shi X, Chen X, Huang W, Liu Y, Liang X, Zhang Z, Su D. Reg3alpha overexpression protects pancreatic beta cells from cytokine-induced damage and improves islet transplant outcome. Mol Med. 2015;20:548–58.
7. Zhang H, Corredor ALG, Messina-Pacheco J, Li Q, Zogopoulos G, Kaddour N, Wang Y, Shi BY, Gregorieff A, Liu JL, Gao ZH. REG3A/REG3B promotes acinar to ductal metaplasia through binding to EXTL3 and activating the RAS-RAF-MEK-ERK signaling pathway. Commun Biol. 2021;4:688.
8. Loncle C, Bonjoch L, Folch-Puy E, Lopez-Millan MB, Lac S, Molejon MI, Chuluyan E, Cordelier P, Dubus P, Lomberk G, et al. IL17 functions through the Novel REG3beta-JAK2-STAT3 inflammatory pathway to promote the transition from chronic pancreatitis to pancreatic cancer. Cancer Res. 2015;75:4852–62.
9. Nigri J, Gironella M, Bressy C, Vila-Navarro E, Roques J, Lac S, Bontemps C, Kozaczyk C, Cros J, Pietrasz D, et al. PAP/REG3A favors perineural invasion in pancreatic adenocarcinoma and serves as a prognostic marker. Cell Mol Life Sci. 2017;74:4231–43.
10. Lai Y, Li D, Li C, Muehleisen B, Radek KA, Park HJ, Jiang Z, Li Z, Lei H, Quan Y, et al. The antimicrobial protein REG3A regulates keratinocyte proliferation and differentiation after skin injury. Immunity. 2012;37:74–84.
11. Marques C, Pocas J, Gomes C, Faria-Ramos I, Reis CA, Vives RR, Magalhaes A. Glycosyltransferases EXTL2 and EXTL3 cellular balance dictates heparan sulfate biosynthesis and shapes gastric cancer cell motility and invasion. J Biol Chem. 2022;298:102546.
12. Avraham R, Yarden Y. Feedback regulation of EGFR signalling: decision making by early and delayed loops. Nat Rev Mol Cell Biol. 2011;12:104–17.
13. Ritchie ME, Phipson B, Wu D, Hu Y, Law CW, Shi W, Smyth GK. limma powers differential expression analyses for RNA-sequencing and microarray studies. Nucleic Acids Res. 2015;43:e47.
14. Mi H, Muruganujan A, Ebert D, Huang X, Thomas PD. PANTHER version 14: more genomes, a new PANTHER GO-slim and improvements in enrichment analysis tools. Nucleic Acids Res. 2019;47:D419–26.
15. Kanehisa M, Furumichi M, Sato Y, Kawashima M, Ishiguro-Watanabe M. KEGG for taxonomy-based analysis of pathways and genomes. Nucleic Acids Res. 2023;51:D587–92.
16. Steele NG, Carpenter ES, Kemp SB, Sirihorachai VR, The S, Delrosario L, Lazarus J, Amir ED, Gunchick V, Espinoza C, et al. Multimodal mapping of the tumor and peripheral blood immune landscape in human pancreatic cancer. Nat Cancer. 2020;1:1097–112.
17. Shiau C, Su J, Guo JA, Hong TS, Wo JY, Jagadeesh KA, Hwang WL. Treatment-associated remodeling of the pancreatic cancer endothelium at single-cell resolution. Front Oncol. 2022;12:929950.
18. Schlesinger Y, Yosefov-Levi O, Kolodkin-Gal D, Granit RZ, Peters L, Kalifa R, Xia L, Nasereddin A, Shiff I, Amran O, et al. Single-cell transcriptomes of pancreatic preinvasive lesions and cancer reveal acinar metaplastic cells' heterogeneity. Nat Commun. 2020;11:4516.
19. Peng J, Sun BF, Chen CY, Zhou JY, Chen YS, Chen H, Liu L, Huang D, Jiang J, Cui GS, et al. Single-cell RNA-seq highlights intra-tumoral heterogeneity and malignant progression in pancreatic ductal adenocarcinoma. Cell Res. 2019;29:725–38.
20. Hao Y, Hao S, Andersen-Nissen E, Mauck WM 3rd, Zheng S, Butler A, Lee MJ, Wilk AJ, Darby C, Zager M, et al. Integrated analysis of multimodal single-cell data. Cell. 2021;184:3573-3587 e3529.
21. Moncada R, Barkley D, Wagner F, Chiodin M, Devlin JC, Baron M, Hajdu CH, Simeone DM, Yanai I. Integrating microarray-based spatial transcriptomics and single-cell RNA-seq reveals tissue architecture in pancreatic ductal adenocarcinomas. Nat Biotechnol. 2020;38:333–42.
22. Van den Berge K, Roux de Bezieux H, Street K, Saelens W, Cannoodt R, Saeys Y, Dudoit S, Clement L. Trajectory-based differential expression analysis for single-cell sequencing data. Nat Commun. 2020;11:1201.
23 Qiu XJ, Mao Q, Tang Y, Wang L, Chawla R, Pliner HA, Trapnell C. Reversed graph embedding resolves complex single-cell trajectories. Nat Methods. 2017;14:979-+.
24. Patel AP, Tirosh I, Trombetta JJ, Shalek AK, Gillespie SM, Wakimoto H, Cahill DP, Nahed BV, Curry WT, Martuza RL, et al. Single-cell RNA-seq highlights intratumoral heterogeneity in primary glioblastoma. Science. 2014;344:1396–401.
25. Aibar S, Gonzalez-Blas CB, Moerman T, Van AHT, Imrichova H, Hulselmans G, Rambow F, Marine JC, Geurts P, Aerts J, et al. SCENIC: single-cell regulatory network inference and clustering. Nat Methods. 2017;14:1083-+.
26. Sun P, Zhu JJ, Wang T, Huang Q, Zhou YR, Yu BW, Jiang HL, Wang HY. Benzbromarone aggravates hepatic steatosis in obese individuals. Biochim Biophys Acta Mol Basis Dis. 2018;1864:2067–77.
27. Zhang J, Li K, Sun HR, Sun SK, Zhu YT, Ge YT, Wu YX, Zhou QY, Li GT, Chang XA, et al. The heparan sulfate mimetic Muparfostat aggravates steatohepatitis in obese mice due to its binding affinity to lipoprotein lipase. Br J Pharmacol. 2023;180:1803–18.
28. Fan Y, Wang J, Jin W, Sun Y, Xu Y, Wang Y, Liang X, Su D. CircNR3C2 promotes HRD1-mediated tumor-suppressive effect via sponging miR-513a-3p in triple-negative breast cancer. Mol Cancer. 2021;20:25.
29. Wang T, Sun P, Chen L, Huang Q, Chen K, Jia Q, Li Y, Wang H. Cinnamtannin D-1 protects pancreatic beta-cells from palmitic acid-induced apoptosis by attenuating oxidative stress. J Agric Food Chem. 2014;62:5038–45.
30. Li K, Qiu C, Sun P, Liu DC, Wu TJ, Wang K, Zhou YC, Chang XA, Yin Y, Chen F, et al. Ets1-mediated acetylation of FoxO1 is critical for gluconeogenesis regulation during feed-fast cycles. Cell Rep. 2019;26:2998-3010 e2995.
31. Kim D, Pertea G, Trapnell C, Pimentel H, Kelley R, Salzberg SL. TopHat2: accurate alignment of transcriptomes in the presence of insertions, deletions and gene fusions. Genome Biol. 2013;14:R36.
32. Berman HM, Westbrook J, Feng Z, Gilliland G, Bhat TN, Weissig H, Shindyalov IN, Bourne PE. The protein data bank. Nucleic Acids Res. 2000;28:235–42.
33. Burley SK, Berman HM, Bhikadiya C, Bi C, Chen L, Di Costanzo L, Christie C, Dalenberg K, Duarte JM, Dutta S, et al. RCSB Protein Data Bank: biological macromolecular structures enabling research and education in fundamental biology, biomedicine, biotechnology and energy. Nucleic Acids Res. 2019;47:D464–74.
34. Desta IT, Porter KA, Xia B, Kozakov D, Vajda S. Performance and its limits in rigid body protein-protein docking. Structure. 2020;28:1071-1081 e1073.
35. Vajda S, Yueh C, Beglov D, Bohnuud T, Mottarella SE, Xia B, Hall DR, Kozakov D. New additions to the ClusPro server motivated by CAPRI. Proteins. 2017;85:435–44.
36. Kozakov D, Hall DR, Xia B, Porter KA, Padhorny D, Yueh C, Beglov D, Vajda S. The ClusPro web server for protein-protein docking. Nat Protoc. 2017;12:255–78.
37. Kozakov D, Beglov D, Bohnuud T, Mottarella SE, Xia B, Hall DR, Vajda S. How good is automated protein docking? Proteins. 2013;81:2159–66.
38. Jones G, Jindal A, Ghani U, Kotelnikov S, Egbert M, Hashemi N, Vajda S, Padhorny D, Kozakov D. Elucidation of protein function using computational docking and hotspot analysis by ClusPro and FTMap. Acta Crystallogr D Struct Biol. 2022;78:690–7.
39. Laskowski RA, Swindells MB. LigPlot+: multiple ligand-protein interaction diagrams for drug discovery. J Chem Inf Model. 2011;51:2778–86.
40. Laskowski RA, Jablonska J, Pravda L, Varekova RS, Thornton JM. PDBsum: structural summaries of PDB entries. Protein Sci. 2018;27:129–34.
41. Zhang G, He P, Tan H, Budhu A, Gaedcke J, Ghadimi BM, Ried T, Yfantis HG, Lee DH, Maitra A, et al. Integration of metabolomics and transcriptomics revealed a fatty acid network exerting growth inhibitory effects in human pancreatic cancer. Clin Cancer Res. 2013;19:4983–93.
42. Yang S, He P, Wang J, Schetter A, Tang W, Funamizu N, Yanaga K, Uwagawa T, Satoskar AR, Gaedcke J, et al. A novel MIF signaling pathway drives the malignant character of pancreatic cancer by targeting NR3C2. Cancer Res. 2016;76:3838–50.
43. Ye Y, Xiao L, Wang SJ, Yue W, Yin QS, Sun MY, Xia W, Shao ZY, Zhang H. Up-regulation of REG3A in colorectal cancer cells confers proliferation and correlates with colorectal cancer risk. Oncotarget. 2016;7:3921–33.
44. Yu LT, Yang MQ, Liu JL, Alfred MO, Li X, Zhang XQ, Zhang J, Wu MY, Wang M, Luo C. Recombinant Reg3alpha protein protects against experimental acute pancreatitis in mice. Mol Cell Endocrinol. 2016;422:150–9.
45. Rosty C, Christa L, Kuzdzal S, Baldwin WM, Zahurak ML, Carnot F, Chan DW, Canto M, Lillemoe KD, Cameron JL, et al. Identification of hepatocarcinoma-intestine-pancreas/pancreatitis-associated protein I as a biomarker for pancreatic ductal adenocarcinoma by protein biochip technology. Cancer Res. 2002;62:1868–75.
46. Zhang MY, Wang J, Guo J. Role of regenerating islet-derived protein 3A in gastrointestinal cancer. Front Oncol. 2019;9:1449.
47. Moniaux N, Geoffre N, Deshayes A, Dos Santos A, Job S, Lacoste C, Nguyen TS, Darnaud M, Friedel-Arboleas M, Guettier C, et al. Tumor suppressive role of the antimicrobial lectin REG3A targeting the O -GlcNAc

glycosylation pathway. Hepatology. 2024. https://doi.org/10.1097/HEP.0000000000000993.
48. Liu X, Wang J, Wang H, Yin G, Liu Y, Lei X, Xiang M. REG3A accelerates pancreatic cancer cell growth under IL-6-associated inflammatory condition: Involvement of a REG3A-JAK2/STAT3 positive feedback loop. Cancer Lett. 2015;362:45–60.
49. Wang YN, Lee HH, Chou CK, Yang WH, Wei Y, Chen CT, Yao J, Hsu JL, Zhu C, Ying H, et al. Angiogenin/Ribonuclease 5 is an EGFR ligand and a serum biomarker for Erlotinib sensitivity in pancreatic cancer. Cancer Cell. 2018;33:752-769 e758.
50. Wang JX, Cao B, Ma N, Wu KY, Chen WB, Wu WJ, Dong X, Liu CF, Gao YF, Diao TY, et al. Collectin-11 promotes cancer cell proliferation and tumor growth. JCI Insight. 2023;8:e159452.
51. Umeda Y, Hasegawa Y, Otsuka M, Ariki S, Takamiya R, Saito A, Uehara Y, Saijo H, Kuronuma K, Chiba H, et al. Surfactant protein D inhibits activation of non-small cell lung cancer-associated mutant EGFR and affects clinical outcomes of patients. Oncogene. 2017;36:6432–45.
52. Mayer S, Raulf MK, Lepenies B. C-type lectins: their network and roles in pathogen recognition and immunity. Histochem Cell Biol. 2017;147:223–37.
53. Krug AW, Schuster C, Gassner B, Freudinger R, Mildenberger S, Troppmair J, Gekle M. Human epidermal growth factor receptor-1 expression renders Chinese hamster ovary cells sensitive to alternative aldosterone signaling. J Biol Chem. 2002;277:45892–7.
54. Calvo F, Sahai E. Cell communication networks in cancer invasion. Curr Opin Cell Biol. 2011;23:621–9.
55. Fukushima N, Koopmann J, Sato N, Prasad N, Carvalho R, Leach SD, Hruban RH, Goggins M. Gene expression alterations in the non-neoplastic parenchyma adjacent to infiltrating pancreatic ductal adenocarcinoma. Mod Pathol. 2005;18:779–87.
56. Albers GH, Escribano MJ, Daher N, Nap M. An immunohistologic study of the feto-acinar pancreatic protein (FAP) in the normal pancreas, chronic pancreatitis, pancreatic adenocarcinoma, and intraabdominal metastases of adenocarcinomas. Am J Clin Pathol. 1990;93:14–9.
57. Hrabak P, Soupal J, Kalousova M, Krechler T, Vocka M, Hanus T, Petruzelka L, Svacina S, Zak A, Zima T. Novel biochemical markers for non-invasive detection of pancreatic cancer. Neoplasma. 2022;69:474–83.
58. O'Brien DP, Sandanayake NS, Jenkinson C, Gentry-Maharaj A, Apostolidou S, Fourkala EO, Camuzeaux S, Blyuss O, Gunu R, Dawnay A, et al. Serum CA19-9 is significantly upregulated up to 2 years before diagnosis with pancreatic cancer: implications for early disease detection. Clin Cancer Res. 2015;21:622–31.
59. Tonack S, Jenkinson C, Cox T, Elliott V, Jenkins RE, Kitteringham NR, Greenhalf W, Shaw V, Michalski CW, Friess H, et al. iTRAQ reveals candidate pancreatic cancer serum biomarkers: influence of obstructive jaundice on their performance. Br J Cancer. 2013;108:1846–53.
60. Xie MJ, Motoo Y, Iovanna JL, Su SB, Ohtsubo K, Matsubara F, Sawabu N. Overexpression of pancreatitis-associated protein (PAP) in human pancreatic ductal adenocarcinoma. Dig Dis Sci. 2003;48:459–64.
61. Wang J, Zhou H, Han Y, Liu X, Wang M, Wang X, Yin G, Li X, Xiang M. SOCS3 methylation in synergy with Reg3A overexpression promotes cell growth in pancreatic cancer. J Mol Med (Berl). 2014;92:1257–69.
62. Parte S, Nimmakayala RK, Batra SK, Ponnusamy MP. Acinar to ductal cell trans-differentiation: a prelude to dysplasia and pancreatic ductal adenocarcinoma. Biochim Biophys Acta Rev Cancer. 2022;1877:188669.

Publisher's Note